

# Vernalization shapes shoot architecture and ensures the maintenance of dormant buds in the perennial *Arabis alpina*

Alice Vayssières<sup>1,2,3</sup> , Priyanka Mishra<sup>1,2,3\*</sup> , Adrian Roggen<sup>1,2,3\*</sup>, Ulla Neumann<sup>3</sup> , Karin Ljung<sup>4</sup>  and Maria C. Albani<sup>1,2,3</sup> 

<sup>1</sup>Institute for Plant Sciences, University of Cologne, Zùlpicher StraÙe 47b, Cologne 50674, Germany; <sup>2</sup>Cluster of Excellence on Plant Sciences 'From Complex Traits towards Synthetic Modules', Düsseldorf 40225, Germany; <sup>3</sup>Max Planck Institute for Plant Breeding Research, Carl-von-Linné-Weg 10, Cologne 50829, Germany; <sup>4</sup>Department of Forest Genetics and Plant Physiology, Umeå Plant Science Centre, Swedish University of Agricultural Sciences, Umeå 90183, Sweden

## Summary

Author for correspondence:

Maria C. Albani

Tel: +49 221 506 2380

Email: [albani@mpipz.mpg.de](mailto:albani@mpipz.mpg.de)

Received: 4 November 2019

Accepted: 29 January 2020

*New Phytologist* (2020) **227**: 99–115

doi: 10.1111/nph.16470

**Key words:** *Arabis alpina*, bud dormancy, dormant bud bank, flowering, perennial, polycarpic, shoot architecture, vernalization.

- Perennials have a complex shoot architecture with axillary meristems organized in zones of differential bud activity and fate. This includes zones of buds maintained dormant for multiple seasons and used as reservoirs for potential growth in case of damage. The shoot of *Arabis alpina*, a perennial relative of *Arabidopsis thaliana*, consists of a zone of dormant buds placed between subapical vegetative and basal flowering branches. This shoot architecture is shaped after exposure to prolonged cold, required for flowering.
- To understand how vernalization ensures the maintenance of dormant buds, we performed physiological and transcriptome studies, followed the spatiotemporal changes of auxin, and generated transgenic plants.
- Our results demonstrate that the complex shoot architecture in *A. alpina* is shaped by its flowering behavior, specifically the initiation of inflorescences during cold treatment and rapid flowering after subsequent exposure to growth-promoting conditions. Dormant buds are already formed before cold treatment. However, dormancy in these buds is enhanced during, and stably maintained after, vernalization by a BRC1-dependent mechanism. Post-vernalization, stable maintenance of dormant buds is correlated with increased auxin response, transport, and endogenous indole-3-acetic acid levels in the stem.
- Here, we provide a functional link between flowering and the maintenance of dormant buds in perennials.

## Introduction

Perennial plants live for many years and reproduce several times during their lifetime, whereas annuals die after the first reproduction. Growth after flowering in perennials is maintained by vegetative meristems, which in the following year will develop either into vegetative branches or stay dormant for multiple seasons. Perennials persist through harsh environmental conditions during the winter. Thus, axillary and apical buds in a perennial plant transition through the various stages of dormancy before they resume active organogenesis the following spring (Rohde & Bhalerao, 2007).

A bud can become dormant and enter a state of low metabolic activity in response to several cues, which is a phenomenon observed in annuals and more often in perennial species. During development, the outgrowth of axillary buds close to the shoot apical meristem is repressed by apical dominance. This is a classic example where the development of an organ is influenced by another organ, and has been described as correlative inhibition,

latency, or paradormancy in annual and perennial species (Cline, 1991; Considine & Considine, 2016). This form of dormancy is not definitive, and buds can resume growth when the inhibiting organ, which is often the main shoot apex, is removed (Snow, 1925). Buds in trees and herbaceous perennials also enter two other forms of dormancy: endo and ecodormancy (Rohde & Bhalerao, 2007). Endodormancy is regulated by endogenous signals within the bud, whereas ecodormancy is imposed by unfavorable environmental conditions (Lang *et al.*, 1987). Thus, ecodormant buds are able to activate growth in response to decapitation (removal of the main shoot apex) only under growth-promotive conditions, whereas endodormant buds are not (Lang *et al.*, 1987). During the life cycle of a perennial plant, apical or axillary buds experience winter in the endodormant state and later become ecodormant, so that they will actively grow only during favorable environmental conditions. However, it is very common in perennials to maintain dormant axillary buds across multiple seasons. These dormant buds serve as a backup bud bank, and in the case of damage they are used as reservoirs for potential growth, facilitating a bet-hedging mechanism (Nilsson *et al.*, 1996; Vasconcelos *et al.*, 2009). Interestingly,

\*These authors contributed equally to this work.

dormant buds and actively growing (vegetative or reproductive) axillary branches are organized in zones in a species-specific pattern (Costes *et al.*, 2014; Lazaro *et al.*, 2018).

The outgrowth of an axillary bud after decapitation involves two phases: first, the rapid release from dormancy; and second, its sustained growth (Wang *et al.*, 2018). Auxin, strigolactones, cytokinin, and sugar fine-tune this process by regulating the expression of the TCP transcription factor BRANCHED 1 (BRC1) (Aguilar-Martínez *et al.*, 2007; Rameau *et al.*, 2015). Decapitation causes an elevation of sucrose levels followed by a depletion of the endogenous indole-3-acetic acid (IAA) in the polar auxin transport stream, which influences the auxin flux out of the axillary bud, contributing to its sustainable growth (Prusinkiewicz *et al.*, 2009; Crawford *et al.*, 2010; Shinohara *et al.*, 2013; Mason *et al.*, 2014; Barbier *et al.*, 2015). The transition to flowering triggers the activation of the uppermost axillary buds in a basipetal sequence having a similar effect to decapitation (Prusinkiewicz *et al.*, 2009; Dierck *et al.*, 2016). In an annual plant, the relation between flowering and bud activation is easy to trace, as its life cycle ends within one growing season. However, many perennials spread the flowering process over several years, and, although they initiate flowering during the summer or autumn, these plants usually flower the following spring (Vasconcelos *et al.*, 2009; Hsu *et al.*, 2011; Kurokura *et al.*, 2013).

Here, we used the perennial *Arabidopsis thaliana*, a close relative of *Arabidopsis thaliana*, to investigate the link between flowering and the maintenance of a dormant bud bank observed in many perennial species. *A. alpina* plants flower in response to prolonged exposure to cold, a process known as vernalization (Wang *et al.*, 2009). Interestingly, floral buds in *A. alpina* are initiated during cold exposure, and the duration of cold treatment is important to ensure floral commitment before plants experience growth-promoting conditions again (Wang *et al.*, 2009; Lazaro *et al.*, 2018). The shoot architecture of *A. alpina* consists of branches that undergo flowering, others that remain vegetative, and nodes with dormant axillary buds (Wang *et al.*, 2009). Similar to other perennials, this architecture is organized in zones, with consequent nodes of dormant axillary buds (V2) being placed between subapical axillary vegetative branches (V3) and basal axillary flowering branches (V1) (Fig. 1; Costes *et al.*, 2014; Lazaro *et al.*, 2018).

As this architecture appears only in plants that flower in response to prolonged cold, we hypothesized that vernalization shapes shoot architecture and the maintenance of dormant axillary buds. We explored this hypothesis by characterizing the zonation pattern of *A. alpina* in conditions that influence flowering. We showed that the zone of V2 dormant buds is present only in flowering plants exposed to a sufficient length of cold treatment that ensures flowering. We also compared the transcriptome of V2 buds with that of V3 buds during and after vernalization. Our analysis indicated that dormancy in V2 buds is enhanced during vernalization and is maintained when plants are returned to growth-promoting conditions. We showed that, during cold exposure, IAA transport in the stem is low and that the growth of V2 buds is inhibited by ecodormancy. V2 axillary

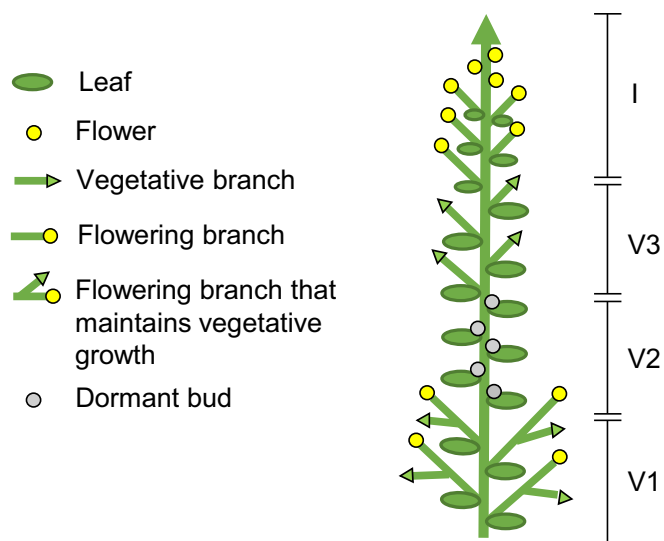


**Fig. 1** Diagram of plant architecture of a flowering *Arabidopsis alpina* wild-type plant. Axillary meristems are organized in zones of differential bud activity and fate: V1, flowering axillary branches that partially senesce; V2, dormant buds; V3, vegetative axillary branches; I, inflorescence. Yellow circle denotes flowering in the inflorescence or axillary branches, gray circles indicate dormant buds, and green triangles indicate the presence of a vegetative branch.

buds stay dormant after plants return to growth-promoting conditions, being dominated by the outgrowing inflorescence and V3 vegetative axillary branches. The *A. alpina* BRC1 also contributes to the maintenance of dormancy in V2 buds, during and after vernalization.

## Materials and Methods

### Plant material, growth conditions, and phenotyping

All our experiments were performed with the *A. alpina* accession Pajares or the *pep1-1* mutant described by Wang *et al.* (2009). Seeds were stratified for 4 d at 4°C and transferred to soil in a long day (LD, 16 h light : 8 h dark) glasshouse at 18–20°C. After 8 wk of growth, cold treatments were carried out in a short day (SD, 8 h light : 16 h dark) growth chamber at 4°C for different durations (depending on the experiment) before plants were moved back to an LD glasshouse. For 1-naphthaleneacetic acid (NAA) and 1-*N*-naphthylphthalamic acid (NPA) treatments, plants were sprayed immediately after 12 wk of cold treatment and 1 wk after the return to an LD glasshouse with 100 μM NAA (Sigma-Aldrich), 100 μM NPA (Chem Service, West Chester, PA, USA), or dimethyl sulfoxide supplemented with 0.2% (v/v) Tween-20. For the simple decapitation method (see Fig. 5), the apex was removed directly above the highest extended internode (corresponding to nodes 11–14 within the V2 zone). Excision of inflorescence and/or V3 buds at the end of vernalization was performed under a stereomicroscope by removing all flowering buds and/or the eight nodes below the lowest flowering bud (corresponding to V3 nodes). The shoot architecture at different time points was scored by recording bud fate (flowering, vegetative, dormant) and branch

length at each node, and the number and types of branches per zone. At least 10–12 plants were used for each experiment.

### Plasmid constructs

The *DR5:GUS* fragment was excised from a plasmid provided by Tom Guilfoyle and introduced into the GATEWAY-compatible pEarleyGate 301 plasmid containing the BASTA resistance gene. For the *35S:AaBRC1* double-stranded RNA interference (*dsRNAi*) constructs, three complementary DNA (cDNA) fragments of *AaBRC1* (fragments 1–3; Supporting Information Table S1) were amplified and introduced into the GATEWAY-compatible pJawohl-8-RNAi plasmid. The names of the *A. alpina* *35S:AaBRC1 dsRNAi* lines correspond to the fragments introduced. For each construct, homozygous transgenic *A. alpina* lines carrying single-copy transgenes were generated using the floral dip method (Clough & Bent, 1998).

### $\beta$ -Glucuronidase staining

V3 buds for the  $\beta$ -glucuronidase (GUS) staining assays were harvested from eight nodes below the lowest flowering bud, whereas V2 buds were harvested from the nodes below to the V3 nodes. V2 stem samples for GUS staining assays were harvested from the upper three extended internodes in the main stem within the V2 zone. Samples were placed directly into 90% ice-cold acetone, incubated for 1 h on ice, washed in 50 mM phosphate buffer (pH 7.0), and submerged in 2.5 ml GUS staining solution under moderate vacuum for 20 min (Scarpella *et al.*, 2004). After a 37°C incubation in the dark for maximum 16 h, chlorophyll was removed by transferring the samples through an ethanol series. GUS activity was observed in whole stem tissues, transverse stem sections, or longitudinal leaf axil sections 50–60  $\mu$ m prepared on a Leica VT1000S (Leica Biosystems, Wetzlar, Germany) vibratome in samples immobilized on 6% (w/v) agarose. Representative photographs from two different biological experiments were taken using a Nikon (Tokyo, Japan) SMZ18 stereomicroscope and Nikon Digital Sight camera (DS-Fi2) for whole stem segments, and a Zeiss Axio Imager microscope with a Zeiss Axio Cam 105 (Zeiss, Jena, Germany) color camera for cuttings.

### RNA extraction, cDNA synthesis, and quantitative real-time PCR

For RNA-sequencing transcript profiling and quantitative reverse transcription (RT)-PCR analysis, V2 and V3 buds were harvested under a stereomicroscope from nodes indicated in each experiment. For quantification of the *GUS* expression of the *DR5:GUS* lines, the upper three extended internodes within the V2 zone in the main stem were harvested and the axillary buds were removed. Each experiment consisted of three independent biological replicates. Total RNA was extracted using the RNeasy Plant Mini Kit (Qiagen) and subjected to DNase treatment using the Ambion DNA-free kit (Invitrogen). Total RNA (2  $\mu$ g) was used for the synthesis of cDNA by reverse transcription with SuperScript II Reverse Transcriptase (Invitrogen) and oligo dT (18) primers.

For quantitative RT-PCR analysis, three technical replicates were prepared using 26 ng of cDNA for each reaction. Relative gene expression values were calculated using  $\Delta C_t$  and the mean of the two reference gene expression values (*AaUBI10* and *AaPP2A*) according to Pfaffl (2001). The  $\Delta C_t$  values were scaled to the average of the control. The primers used are listed in Table S1.

### RNA-sequencing transcript profiling

Poly(A) RNA enrichment, library preparation, and sequencing were carried out at the MPIPZ Genome Center, Cologne, Germany, using 1  $\mu$ g total RNA. Poly(A) RNA was isolated using the NEBNext Poly(A) mRNA Magnetic Isolation Module (New England Biolabs, Ipswich, MA, USA) and quantified using capillary electrophoresis (TapeStation; Agilent Technologies, Santa Clara, CA, USA) and a fluorometer (Qubit; Thermo Fisher Scientific, Waltham, MA, USA). Libraries were prepared using the NEBNext Ultra Directional II RNA Library Prep Kit for Illumina (New England Biolabs, Ipswich, MA, USA) and sequenced using a HiSeq3000 (Illumina) with 1  $\times$  150 bp single read length.

Sequence reads were mapped and aligned to the reference genome using HISAT2 followed by assembly and quantification of expression levels using STRINGTIE. Gene counts for all samples were obtained using Python (<http://ccb.jhu.edu/software/stringtie/dl/prepDE.py>). The quality of the samples was assessed using dispersion plots. Differentially expressed genes with more than two-fold change and a corrected *P*-value < 0.05 were obtained using DESEQ2 and selected for further analysis. Transcriptome data from this study are deposited in the Gene Expression Omnibus database (<http://www.ncbi.nlm.nih.gov/geo/>) under accession no. GSE126944. Gene Ontology (GO) enrichment was performed using DAVID (Huang *et al.*, 2009) for biological processes 5, with Benjamini correction (*P* value < 0.05) and plotted using the BACA package in R (Fortino & Greco, 2015; <http://r-project.org/>) only for the Arabidopsis annotated orthologues. Data were analyzed using hierarchical clustering. Fragments per kilobase of transcript per million mapped reads (FPKM) values were extracted from the STRINGTIE-created GTF files and  $\log_2$  transformed. For the clustering we used CLUSTER 3.0, in which we included only the genes that met both of the following criteria: (1) a  $\log_2$  FPKM value  $\geq 2$  in at least one sample; (2) a difference between the maximum and minimum expression value of  $\geq 1.5$ . The  $\log_2$  FPKM values of selected genes were median centered by transcript. Hierarchical clustering was performed using uncentered correlation and average linkage. Data were visualized using Java TREEVIEW (<http://doi.org/10.5281/zenodo.1303402>). Venn diagrams were constructed using VENNY v.2.1 (<http://bioinfogp.cnb.csic.es/tools/venny/>).

### Quantification of IAA

For the free IAA quantification of V2 samples, the upper three extended internodes within the V2 zone in the main stem were harvested and the axillary buds were removed. For the free IAA quantification of inflorescence (I) and V3 branches, 2 cm stem cuttings from the base of each branch were harvested. Plant

material (15 mg fresh weight) was purified as previously described in Andersen *et al.* (2008), and 500 pg  $^{13}\text{C}_6$ -IAA internal standard was added to each sample before homogenization and extraction. Free IAA was quantified in the purified samples using combined gas chromatography–tandem mass spectrometry.

### $^3\text{H}$ -IAA transport assay

For the auxin transport capacity assay, we harvested the top elongated stem segment within the V2 zone (21 mm) from plants after 8 wk in LDs (8wLD), after 12 wk cold treatment (+0), and 5 d after the return to LD glasshouse conditions (+5d). Stem segments were placed on wet paper and transferred to 30  $\mu\text{l}$  0.05% Mes (pH 5.5–5.7) containing 100 nM  $^3\text{H}$ -IAA with the apical part being submerged into the solution for 10 min (Hartmann Analytic GmbH, Braunschweig, Germany). Samples were then transferred to fresh 0.05% MES containing 1  $\mu\text{M}$  IAA for 90 min (Lewis & Muday, 2009). Samples harvested at the end of cold treatment were incubated with 1  $\mu\text{M}$  IAA at 4°C. Subsequently, samples were cut into 3 mm segments, with 0–3 mm being the apical part of the sample, and immersed in Rotiszint eco plus (Carl Roth, Karlsruhe, Germany) for 16 h before the quantification by scintillation for 2 min using an LS6500 multipurpose scintillation counter (Beckman Coulter, Brea, CA, USA). Counts per minute values were scaled to the average for the 8wLD samples at 6–9 mm or for 8wLD total samples.

### Statistical analysis

Data were analyzed using ANOVA followed by a Tukey post hoc test for pairwise multiple comparisons using the R platform (<http://r-project.org/>). Pairwise comparisons were analyzed using Student's *t*-test.

## Results

Vernalization in *A. alpina* correlates with the formation of a complex shoot architecture and the maintenance of dormant buds

The *A. alpina* accession Pajares flowers in response to prolonged cold treatment (Wang *et al.*, 2009). We scored bud activity and fate in Pajares (wild-type) plants grown in LDs for 8 wk (8wLD), exposed to 12 wk cold treatment (+0) and subsequently returned back to an LD glasshouse for up to 9 wk (Fig. 2a–f). Plants before cold treatment developed axillary vegetative branches only in the lower nodes (1–8), whereas upper nodes (9–21) contained dormant buds (Fig. 2e; 8wLD; Ponraj & Theres, 2020). After cold treatment, plants flowered and already at 3 wk post-vernalization had established a complex architecture consisting of basal flowering and vegetative axillary branches (Fig. 2a,b; the yellow and the green boxes in nodes 1–12 in Fig. 2e), subapical vegetative axillary branches (Fig. 2b; the green boxes in nodes 22–29 in Fig. 2e), and apical inflorescence branches (Fig. 2a; the yellow boxes in nodes 30–40 in Fig. 2e). Basal flowering branches differ from the inflorescence branches by only partially senescing at the

end of flowering. Nodes 13–21 were not occupied by an axillary branch or contained a bud that did not grow > 0.5 cm even after 9 wk post-vernalization (Fig. 2c,d; the gray and the brown boxes in Fig. 2e). This result suggests that buds in nodes 13–21 are dormant before and after cold treatment. Similar to other woody perennials, the *A. alpina* stem was organized in zones of differential bud activity and fate according to their position on the main stem (Figs 1, 2e; Costes *et al.*, 2014; Lazaro *et al.*, 2018). Nodes 13–21 represent the V2 dormant bud zone and were the last nodes initiated before cold treatment. This zone is located between the subapical V3 zone of axillary vegetative branches (nodes 22–29) and the V1 zone of basal flowering branches (nodes 1–12) (Figs 1, 2e; Lazaro *et al.*, 2018).

To check whether this architecture is determined by vernalization response, we scored the shoot architecture in the *perpetual flowering 1* (*pep1*) mutant, which carries lesions in the orthologue of the MADS box transcription factor FLOWERING LOCUS C (FLC) and does not require cold treatment to flower (Michaels & Amasino, 1999; Sheldon *et al.*, 2000; Wang *et al.*, 2009). All axillary buds in *pep1-1* developed into flowering branches and, similar to wild-type plants, were activated acropetally (Fig. 2f,g; Wang *et al.*, 2009). *pep1-1* also lacked the zones of dormant axillary buds and vegetative axillary branches. In wild-type plants, buds were gradually activated in an acropetal manner, giving rise to an axillary branch even in nodes that stay stably dormant after exposure to cold treatment (Fig. 2g). This result suggests that vernalization in *A. alpina* is required to ensure the stable maintenance of dormant buds.

To further assess the relationship between vernalization and shoot architecture, we exposed wild-type plants to an insufficient duration of cold treatment that does not ensure flowering and scored bud activity and fate (Fig. 3). Similar to previous studies, plants grown continuously in LDs or cold treated only for 3 wk did not flower, whereas plants exposed to 8 wk cold treatment showed extreme floral reversion phenotypes (e.g. inflorescences produced leaves instead of flowers) (Fig. S1; Wang *et al.*, 2009; Lazaro *et al.*, 2018). We compared the length of axillary branches at each leaf axil at 3 wk after cold treatment or after 11 wk in LDs for the non-cold-treated plants. Branch length in LD-grown plants and in plants exposed to 3 wk of cold was reduced acropetally (treatments 0 and 3 in Fig. 3c). Interestingly, nodes 13–19 (corresponding to the V2 zone) were completely inhibited only in plants exposed to 12 wk of cold and which flowered (treatment 12 in Fig. 3b,c). In plants exposed to 8 wk of cold treatment, axillary branches developed in nodes 13–19 (V2 zone) but their length was shorter than branches in nodes 1–12 (V1 zone) or in nodes 20–29 (V3 zone) (treatment 8 in Fig. 3b,c). Interestingly, V3 vegetative branches appeared only in flowering plants and were always located just above the nodes with the inhibited buds. This result suggests that the presence of V3 branches might be correlated with the repression of bud growth in the V2 zone, but only a period of 12 wk of cold treatment secures the stable inhibition of V2 buds.

Overall, these results suggest that vernalization is linked to the complex architecture in *A. alpina*, and genotypes that flower without cold treatment lack the zone of dormant buds.



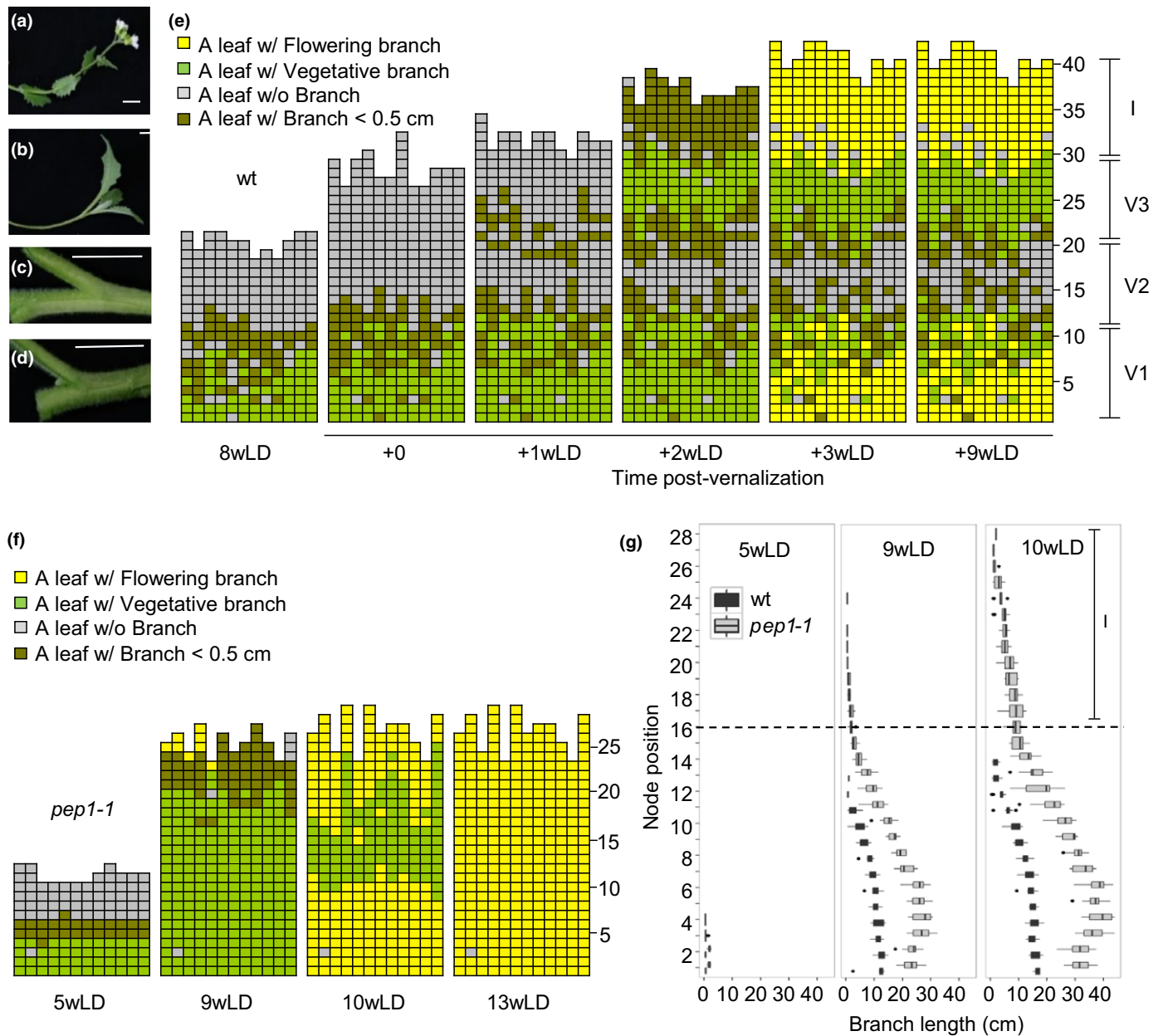


**Fig. 2** Vernalization determines shoot architecture in *Arabis alpina*. (a–e) Analysis of branch formation in wild-type (wt) Pajares plants cold treated for 12 wk. (a) A flowering branch. (b) A vegetative branch. (c) A leaf axil without a branch. (d) A leaf axil with a branch smaller than 0.5 cm. Bars, 1 cm. (e) Analysis of branch formation in a set of wt plants grown in long days (LDs) for 8 wk (8wLD), cold treated for 12 wk (+0), and transferred back to LDs for 1, 2, 3, and 9 wk (+1wLD, +2wLD, +3wLD, and +9wLD). Zones are mentioned on the right as described in Fig. 1. (f, g) Analysis of branch formation in *pep1-1* mutant growing continuously in LDs. (f) Analysis of branch formation in a set of *pep1-1* plants scored for up to 13 wk (5wLD, 9wLD, 10wLD and 13wLD) in an LD glasshouse. (g) Branch length in each node in *pep1-1* and wt plants. In (e) and (f) each column represents a single plant, and each square within a column represents an individual leaf axil numbered from the oldest to the youngest node. Yellow or green colors indicate the presence of a flowering (as in a) or vegetative axillary branch (as in b) in the particular leaf axil. Gray or brown colors indicate the absence of an axillary branch (as in c) or the presence of a branch smaller than 0.5 cm (as in d) in the particular leaf axil.  $n = 12$ . In (g) the boxes indicate the interquartile range, the vertical line in the middle is the median, the horizontal lines (whiskers) correspond to the highest or lowest value within 1.5 times the interquartile range, and the dots are outliers.

Transcriptome analysis suggests that V3 buds are not dormant during vernalization, whereas dormancy in V2 buds is ensured during and after vernalization

To investigate the molecular mechanisms that lead to the activation of V3 buds and the inhibition of growth in V2 buds, we

performed a transcriptome profiling. To identify an early developmental stage post-vernalization in which the V2 and V3 buds are differentiated, we developed transgenic *A. alpina* plants carrying the *DR5* promoter fused to the reporter gene *GUS*. In *A. thaliana* and other species, bud growth has been demonstrated using the auxin-inducible synthetic promoter *DR5*

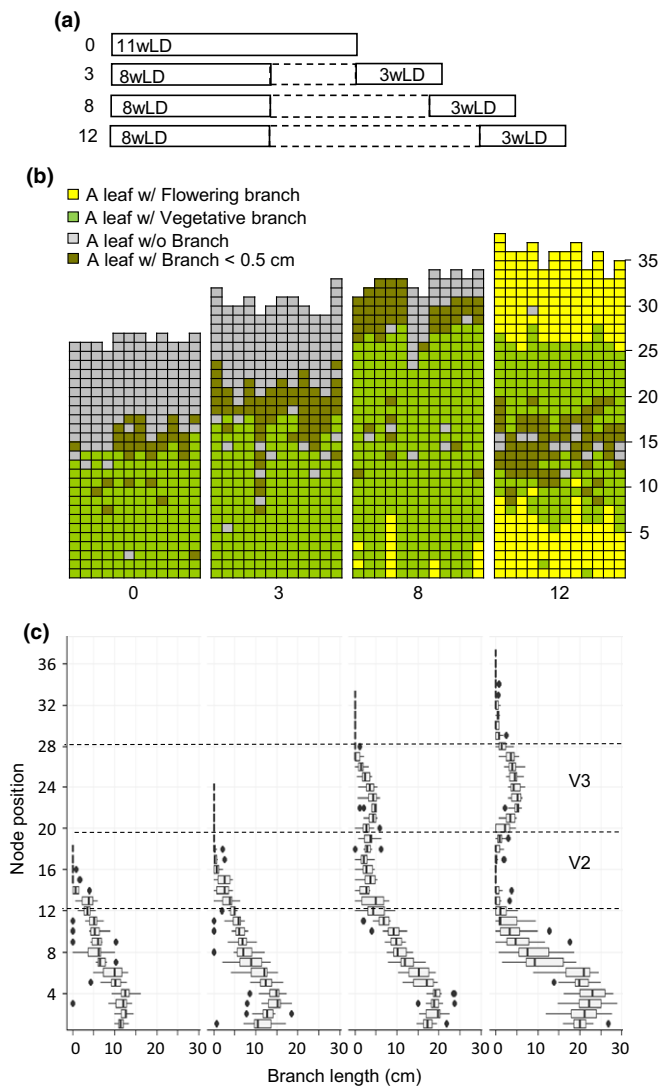


**Fig. 3** The duration of cold treatment in *Arabis alpina* determines shoot architecture and the maintenance of a zone of dormant buds. (a) Diagram illustrating the experimental design. Plants were grown for 11 wk in long days (LDs) (0), or for 8 wk in LDs and subsequently cold treated for 3 wk (3w), 8 wk (8w), or 12 wk (12w). Plants were scored 3 wk after they were returned to an LD glasshouse. Solid line box represents LD glasshouse conditions, and dotted line box vernalization at 4°C under short days. (b) Analysis of branch formation in plants exposed to different durations of cold treatment or to continuous LDs for 11 wk. As in Fig. 2, each column represents a single plant and each square within a column represents an individual leaf axil numbered from the oldest to the youngest node. Yellow or green colors indicate the presence of a flowering or vegetative axillary branch in the particular leaf axil. Gray or brown colors indicate the absence of an axillary branch or the presence of a branch smaller than 0.5 cm in the particular leaf axil. (c) Branch length of axillary branches in each node in plants exposed to different durations of cold treatment or to continuous LDs for 11 wk. The boxes in (c) indicate the interquartile range, the vertical line in the middle is the median, the horizontal lines (whiskers) correspond to the highest or lowest value within 1.5 times the interquartile range, and the dots are outliers. Nodes corresponding to V2 and V3 zones are indicated.  $n = 12$ .

(Prusinkiewicz *et al.*, 2009; Barbier *et al.*, 2015). In *A. alpina* DR5:GUS transgenic plants, we detected the GUS signal only in V3 buds at 5 d post-vernalization (Fig. 4a–d). This result suggests

that, although at 5 d post-vernalization there is no obvious development of V3 branches, the growth of V3 buds is activated. We then harvested axillary buds from nodes 16–19 to represent V2 buds and axillary buds from nodes 23–26 to represent V3 buds. Buds were harvested from plants immediately after 12 wk of cold treatment (+0) and 5 d post-vernalization (+5d). As expected, the transcriptome of V2 and V3 buds at 5 d post-vernalization was the most dissimilar (1984 genes; +5dV2 vs +5dV3; Fig. 4e; Table S2). Interestingly, the transcriptome of V2 and V3 buds also differed at the end of vernalization (1128 genes for +0V2 vs +0V3; Fig. 4e; Table S2), suggesting that the V2 and V3 buds were already differentiated during cold treatment. Almost all genes that were differentially expressed between V2 and V3 buds at the end of cold treatment were also differentially expressed in the other comparisons (Fig. 4e). Likewise, GO enrichment analysis indicated that all GOs enriched for the differentially expressed genes between V2 and V3 buds at the end of cold treatment were also identified in the other comparisons (Fig. S2; Table S3). GO terms common to all comparisons were mainly associated with ‘water deprivation’ and ‘hormone responses’, such as abscisic acid (ABA), ethylene, and jasmonic acid.

To identify genes that share similar expression patterns, we performed hierarchical clustering analysis. Low-expressed and invariant genes were filtered out, and 4983 genes could be classified using hierarchical clustering from the 25 817 whose transcripts were found accumulated in at least one of the conditions tested (Fig. 4f). Our biological replicates were clustered together (Fig. 4f). Interestingly, samples harvested at the end of cold treatment (+0) were separated from samples harvested from plants 5 d after the return to glasshouse conditions (+5d), suggesting a general transcriptional reprogramming in both V2 and V3 buds when plants were moved from cold to warm conditions (Fig. 4f). We identified 34 coexpressed clusters, which were assigned into two higher level clusters I and II (Fig. 4f; Table S4). The separation of these higher level clusters was shaped by the expression of genes in the V3 buds during vernalization. Genes in clusters I and II showed low and high transcript accumulation, respectively, in V3 buds at the end of vernalization (Fig. 4f). Genes in clusters I3 and I6 showed higher transcript accumulation in V3 buds post-vernalization, accounting for putative candidate genes involved in the activation of growth in V3 buds (Fig. 4g,h). These included homologues of genes involved in cell expansion *EXPANSIN B1*, IAA biosynthesis *YUCCA2*, and the auxin signaling factors *INDOLE-3-ACETIC ACID 7* and *14* (Fig. 4g,h; Zhao *et al.*, 2001; Sharova, 2007; Paponov *et al.*, 2008). Interestingly, most enriched GO terms in cluster I3 were associated with developmental processes (e.g. ‘trichome differentiation’, ‘plant epidermis morphogenesis’, and ‘cell fate commitment’) (Table S5). Genes in clusters II7 and II8 already showed higher transcript accumulation in V3 buds compared with V2 buds during cold treatment (Fig. 4j). Both clusters were enriched for GO terms related to cell division (e.g. ‘DNA metabolic processes’, ‘DNA replication’, and ‘nuclear division’) and included cell cycle regulators, such as *PROLIFERATING CELLULAR NUCLEAR ANTIGEN 1*, shown to be upregulated during bud activation in other species (Fig. 4j; Tables S4, S5; Roman *et al.*, 2016; Holalu

& Finlayson, 2017). The enrichment of genes involved in cell cycle and transcriptional machinery detected to be upregulated in V3 buds during vernalization suggests that V3 buds are not dormant during cold treatment.

Clusters I14, I15, I20, and I21 showed higher transcript accumulation in V2 buds compared with V3 buds during and after cold treatment (Fig. 4i). Interestingly, all these clusters were enriched for GOs related to ABA and water deprivation (Fig. 4i; Table S5). These clusters contained genes related to ABA signaling, such as *ABA INSENSITIVE RING PROTEIN 2* (*AIRP2*), *ABSCISIC ACID RESPONSIVE ELEMENT-BINDING FACTOR 1* and *2*, *ABA INSENSITIVE 1* and *5* (*ABI1*, *ABI5*), *KINASE 2*, *ABI FIVE BINDING PROTEIN 1* and *3*, *BELI-LIKE HOMEODOMAIN 1*, and *PROTEIN PHOSPHATASE 2CA*, or ABA biosynthesis (e.g. *NINE-CIS-EPOXYCAROTENOID DIOXYGENASE 3*) shown to be associated with bud dormancy in several species (Fig. 4i; Destefano-Beltrán *et al.*, 2006; Zheng *et al.*, 2015; Chao *et al.*, 2017; Singh *et al.*, 2018). We also detected the dehydrin coding genes *EARLY RESPONSIVE TO DEHYDRATION 10* and *14* and *RESPONSIVE TO ABA 18*, which are induced by ABA and suggested to prevent water dehydration during tree winter dormancy (Fig. 4i; Arora *et al.*, 2003). Transcript accumulation of homologues of genes associated with the repression of the cytokinin level and response such as *CYTOKININ OXIDASE/DEHYDROGENASE 1* and *KISS ME DEADLY 1–4* were also detected in these clusters (Fig. 4i; Werner *et al.*, 2001; Kim *et al.*, 2013). We also identified the homologues of genes that have been previously shown in *A. thaliana* to respond to conditions that trigger dormancy and which, therefore, are considered as dormancy markers (Taracón *et al.*, 2017). This includes the *A. alpina* homologues of *HOMEODOMAIN 21* and *53* (*HB21*, *HB53*), *PLANT PEPTIDE CONTAINING SULFATED TYROSINE 1*, *NAC DOMAIN CONTAINING PROTEIN 29* (*NAC029*), *SENESCENCE-ASSOCIATED GENE 21*, *HISTONE H1-3* (*HIS1-3*), and *EIN3-BINDING F BOX PROTEIN 2* (genes highlighted in bold in Fig. 4i; Table S6). Interestingly, genes in cluster I21 showed high transcript upregulation in V2 buds specifically post-vernalization (Fig. 4i). In this cluster, we detected the homologues of the strigolactone signaling genes *DWARF 14* (*D14*) and *SUPPRESSOR OF MAX2 1*. *D14* in *A. thaliana* and its homologues in other species regulate bud dormancy (Arite *et al.*, 2009; Waters *et al.*, 2012). Overall, these results suggest that dormancy in V2 buds is regulated during and after vernalization and involved in the activation of ABA and strigolactone signaling genes.

## V2 buds become ecodormant during cold exposure and are under the control of correlative inhibition after plants return to growth-promoting conditions

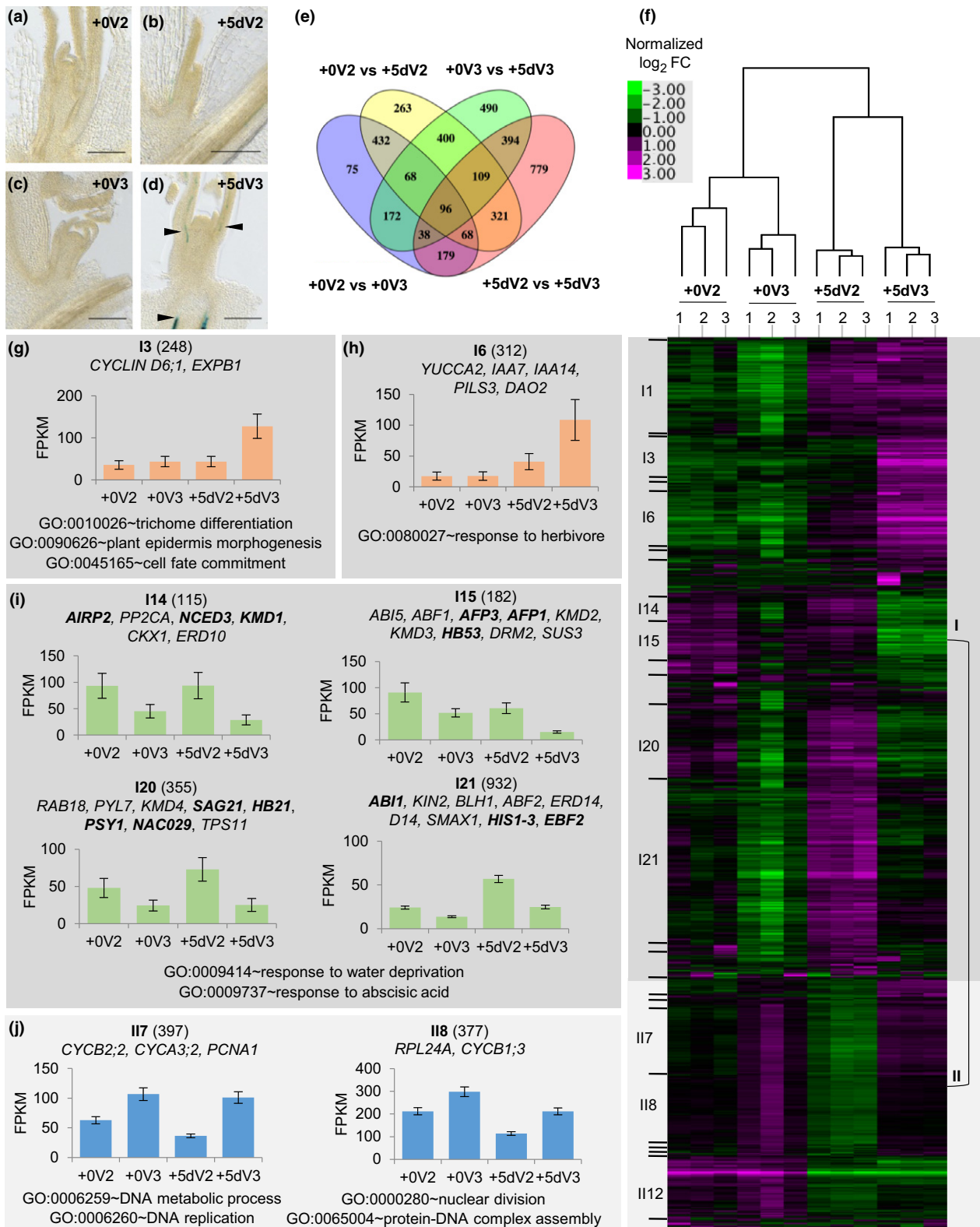
To assess whether cold imposes an endodormant or ecodormant state on V2 buds, we decapitated plants immediately after being exposed to different durations of cold treatment by removing the primary stem above nodes 11–14, depending on the treatment (Fig. 5a). Plants cold treated for < 12 wk failed to maintain dormant buds even in nondecapitated controls (Fig. 5c). Irrespective of the cold treatment, the length of axillary branches that developed after plants returned to glasshouse conditions was longer in

decapitated plants compared with nondecapitated controls (Fig. 5b). Endodormant buds do not respond to decapitation (Lang *et al.*, 1987); therefore, we conclude that V2 buds are not endodormant during cold treatment. To assess the effect of cold on bud outgrowth, we decapitated plants and exposed them to 12 wk of cold treatment (Fig. 5d–f). Buds in decapitated and intact plants did not grow during cold treatment, suggesting that cold inhibits growth and imposes an ecodormant state in V2 buds (Fig. 5e,f).

Since V2 buds also remain dormant after plants return to growth-promoting conditions, we tested whether the outgrowth of V2 buds post-vernalization is determined by other parts of the plant (Fig. 6a). For this, we performed a series of decapitation and excision experiments by excising buds or branches in vernalized plants before returning to the glasshouse (Fig. 6a). Excision of the inflorescence buds (I) or V1 branches separately reduced the number of dormant buds in the V2 zone (nodes 11–16; Fig. 6a,b). The biggest effect on bud outgrowth in the V2 zone was obtained when we excised both inflorescence and V3 buds (I + V3) together (Fig. 6a,b). These results suggest that the outgrowth of buds within the V2 zone post-vernalization is influenced by other parts of the plant.

To validate that the genes we identified in our transcriptome profiling regulate dormancy in V2 buds, we tested their expression patterns after decapitation (Fig. 6c). For this, we vernalized plants and removed the inflorescence and V3 buds (I + V3) before transferring them back to glasshouse conditions. Transcript accumulation of selected genes was tested in the axillary buds within the V2 zone at 5 d after the excision of the inflorescence and V3 buds (I + V3). Decapitation resulted in a reduced transcript level of all genes tested. This result suggests that the expression of these genes post-vernalization is regulated by an apical signal (Fig. 6c).

In many species, bud inhibition by apical dominance is regulated by polar auxin transport (Wang *et al.*, 2018). We performed several tests to assess whether changes in auxin dynamics are important for the maintenance of dormancy in V2 buds post-vernalization (e.g. we measured endogenous IAA levels, auxin response, and auxin transport). We first tested auxin response in the topmost elongated internodes within the V2 region of the main stem using the *DR5:GUS* transgenic *A. alpina* plants. We decapitated plants immediately after 12 wk of cold treatment and afterwards transferred them to glasshouse conditions. Stems from decapitated plants at 5 d post-vernalization (Figs 7c,f, S3) and intact plants at the end of cold treatment (Figs 7a,d, FS3) did not show a strong GUS signal. By contrast, we detected a GUS signal in nondecapitated plants 5 d post-vernalization (Figs 7b,e, S3). This result suggests that auxin response is enhanced in the V2 region of the main stem post-vernalization. We also measured the levels of endogenous IAA during the *A. alpina* life cycle. Similar to *DR5:GUS* results, IAA levels in the main stem (in the internodes within the V2 region) were low during vernalization and were transiently increased post-vernalization (Fig. 7g). Interestingly, IAA levels at 2 wk post-vernalization were very high, which correlated with high IAA levels in the stems of the actively growing inflorescence stems (Fig. 7h) and V3 branches (Fig. 7i).



Decapitation by removal of the inflorescence and V3 buds (I + V3) at the end of cold treatment did not result in an increase of the endogenous IAA levels in the V2 stem measured 5 d post-vernalization (Fig. 7j). This result suggests that the outgrowth of

the inflorescence and V3 branches post-vernalization induces a higher IAA level in the V2 main stem. To test whether the transient increase of the endogenous IAA level in the stem represents an increase in auxin transport, we measured IAA transport



**Fig. 4** The transcriptomes of V2 and V3 buds are already differentiated during vernalization. (a–d)  $\beta$ -Glucuronidase (GUS) activity in longitudinal sections of axillary buds harvested from the nodes in V2 and V3 zones in *DR5:GUS Arabis alpina* plants. (a) V2 buds at the end of 12 wk of vernalization (+0). (b) V2 buds 5 d post-vernalization (+5d). (c) V3 buds at the end of 12 wk of vernalization (+0). (d) V3 buds 5 d post-vernalization (+5d). Arrows indicate GUS signal. Bars, 250  $\mu$ m. (e) Venn diagram showing the overlap of significantly regulated genes in V2 and V3 buds at the end of vernalization (+0) and 5 d post-vernalization (+5d). (f) Heat map representing the hierarchical clustering of 4983 coexpressed transcripts between samples. Coexpressed clusters were assigned into two higher level clusters (I and II). (g–j) Expression profiles of selected clusters using fragments per kilobase of transcript per million mapped reads (FPKM) values. Error bars represent the SE of all FPKM values of genes within the cluster obtained in a particular sample. (g, h) Clusters that show higher transcript accumulation only in V3 buds post-vernalization. (i) Clusters that show higher transcript accumulation in V2 buds during and after vernalization. (j) Clusters that show higher transcript accumulation in V3 buds during and after vernalization. The selected Gene Ontology (GO) terms shown in (g) and (h) are predominant in each cluster. The selected GO terms shown in (i) and (j) are representative and shared between clusters in each group. Selected GO terms had *P*-values after Benjamini correction lower than 0.05. Numbers in parentheses indicate the number of genes present in each cluster. Above each cluster, selected representative genes that belong to common GOs and which are related to development or dormancy are indicated. Genes highlighted in bold were suggested in Tarancon *et al.* (2017) to be *bud dormancy* genes as their expression patterns are correlated with bud dormancy. *ABF1* and *ABF2*, *ABSCISIC ACID RESPONSIVE ELEMENT-BINDING FACTOR 1* and *2*; *ABI1* and *ABI5*, *ABA INSENSITIVE 1* and *5*; *AFP1* and *AFP3*, *ABI FIVE BINDING PROTEIN 1* and *3*; *AIRP2*, *ABA INSENSITIVE RING PROTEIN 2*; *BLH1*, *BEL1-LIKE HOMEODOMAIN 1*; *CKX1*, *CYTOKININ OXIDASE/DEHYDROGENASE 1*; *D14*, *DWARF 14*; *DAO2*, *DIOXYGENASE FOR AUXIN OXIDATION 2*; *EBF2*, *EIN3-BINDING F BOX PROTEIN 2*; *ERD10* and *ERD14*, *EARLY RESPONSIVE TO DEHYDRATION 10* and *14*; *EXPB1*, *EXPANSIN B1*; *HB21* and *HB53*, *HOMEODOMAIN 21* and *53*; *HIS1-3*, *HISTONE H1-3*; *IAA7* and *IAA14*, *INDOLE-3-ACETIC ACID 7* and *14*; *KIN2*, *KINASE 2*; *KMD1-4*, *KISS ME DEADLY 1-4*; *NACO29*, *NAC DOMAIN CONTAINING PROTEIN 29*; *NCED3*, *NINE-CIS-EPOXYCAROTENOID DIOXYGENASE 3*; *PCNA1*, *PROLIFERATING CELLULAR NUCLEAR ANTIGEN 1*; *PILS3*, *PIN-LIKES 3*; *PP2CA*, *PROTEIN PHOSPHATASE 2CA*; *PSY1*, *PLANT PEPTIDE CONTAINING SULFATED TYROSINE 1*; *PYL7*, *PYRABACTIN RESISTANCE-LIKE 7*; *RAB18*, *RESPONSIVE TO ABA 18*; *SAG21*, *SENESCENCE-ASSOCIATED GENE 21*; *SMAX1*, *SUPPRESSOR OF MAX2 1*; *TPS11*, *TREHALOSE-6-PHOSPHATE SYNTHASE 11*.

capacity using acropetal  $^3\text{H}$ -IAA treatment in excised stem segments of the main stem corresponding to the V2 region. We compared the same V2 stem region from plants grown for 8 wk in an LD glasshouse (8wLD), after 12 wk of cold treatment (+0), and subsequently after 5 d in glasshouse conditions (+5d).  $^3\text{H}$ -IAA levels in the V2 zone were higher before and after vernalization, compared with at the end of vernalization (Fig. 7m,n). This result suggests that prolonged exposure to cold leads to a decrease in auxin transport in the V2 zone that is re-established after the return to growth-promoting conditions. We finally applied the synthetic auxin NAA and the auxin transport inhibitor NPA to plants cold-treated for 12 wk before being transferred back to the glasshouse. NAA treatment increased and NPA treatment reduced the number of buds in the V2 zone compared with mock-treated plants (Fig. 7o,p). In addition, NPA strongly impaired the development of the inflorescence and V1 branches (Fig. 7p). These results confirmed the importance of auxin levels and auxin transport for the inhibition of buds in the V2 zone post-vernalization.

Altogether, we conclude that the outgrowth of the inflorescence and of the V3 vegetative branches post-vernalization correlates with an enhancement of endogenous IAA levels and auxin response and transport in the V2 zone, which may stably repress the outgrowth of V2 buds. During cold treatment, although auxin transport is low, the development of V2 axillary buds is inhibited by ecodormancy.

#### AaBRC1 ensures the maintenance of dormancy in V2 buds post-vernalization

As *BRC1* (and to a lesser extent *BRC2*) are the major regulators of bud dormancy in *A. thaliana*, we also followed the expression patterns of their homologues (*AaBRC1* and *AaBRC2*) in *A. alpina* (Fig. S4; Aguilar-Martínez *et al.*, 2007; González-Grandío *et al.*, 2013). *AaBRC1* transcript levels were higher in V2 buds than in V3 buds 5 d after vernalization (Fig. S4b).

Similar to the expression patterns of the genes detected in our transcriptome, *AaBRC1* transcript levels in V2 buds were reduced in response to decapitation (Figs 6c, S4b). *AaBRC2* expression levels did not differ between V2 and V3 buds and in response to decapitation (Fig. S4b). We subsequently tested the expression of candidate genes from our transcriptome and *AaBRC1* on V2 buds across the *A. alpina* life cycle. Buds from the V2 zone (nodes 17–20) were harvested from plants at different developmental stages, after being grown for 8 wk in an LD glasshouse (8wLD), cold-treated for 12 wk (+0), and subsequently transferred back to an LD glasshouse for 5 d (+5d). *AaBRC1* transcript levels in V2 buds increased during cold treatment and remained at a high level after plants were returned to glasshouse conditions (Fig. 8). This expression pattern was shared for most genes tested, including the *A. alpina* homologue of *HB53* (*AaHB53*), which is a direct target of *BRC1* in *A. thaliana* (González-Grandío *et al.*, 2017). Interestingly, transcript accumulation of *AaHIS1-3*, which in *A. thaliana* has a *BRC1*-dependent expression pattern, increased only post-vernalization (Fig. 8). These results suggest that dormancy in V2 buds is enhanced during vernalization and is maintained post-vernalization after plants experience growth-promoting conditions.

We also created transgenic lines with reduced expression of *AaBRC1*. Plants of *35S:AaBRC1 dsRNAi* lines 1 and 2 showed significant downregulation of *AaBRC1* expression, whereas line 3 did not (Fig. S5). We characterized these lines at different developmental stages with plants grown for 8 wk in LDs (8wLD), exposed to 12 wk of cold treatment (+0), and subsequently returned to an LD glasshouse for 5 wk (+5w) (Fig. 9). Before vernalization, we observed no difference in branch number and branch length (Figs 9a–c, S6a). Transgenic lines also flowered with a similar total number of leaves compared with control plants (Fig. S6d–h). Lines 1 and 2 showed a minor difference in branch number at the end of vernalization (Fig. 9a,c). The branching phenotype in lines 1 and 2 became stronger post-vernalization and showed an increased number of branches in nodes

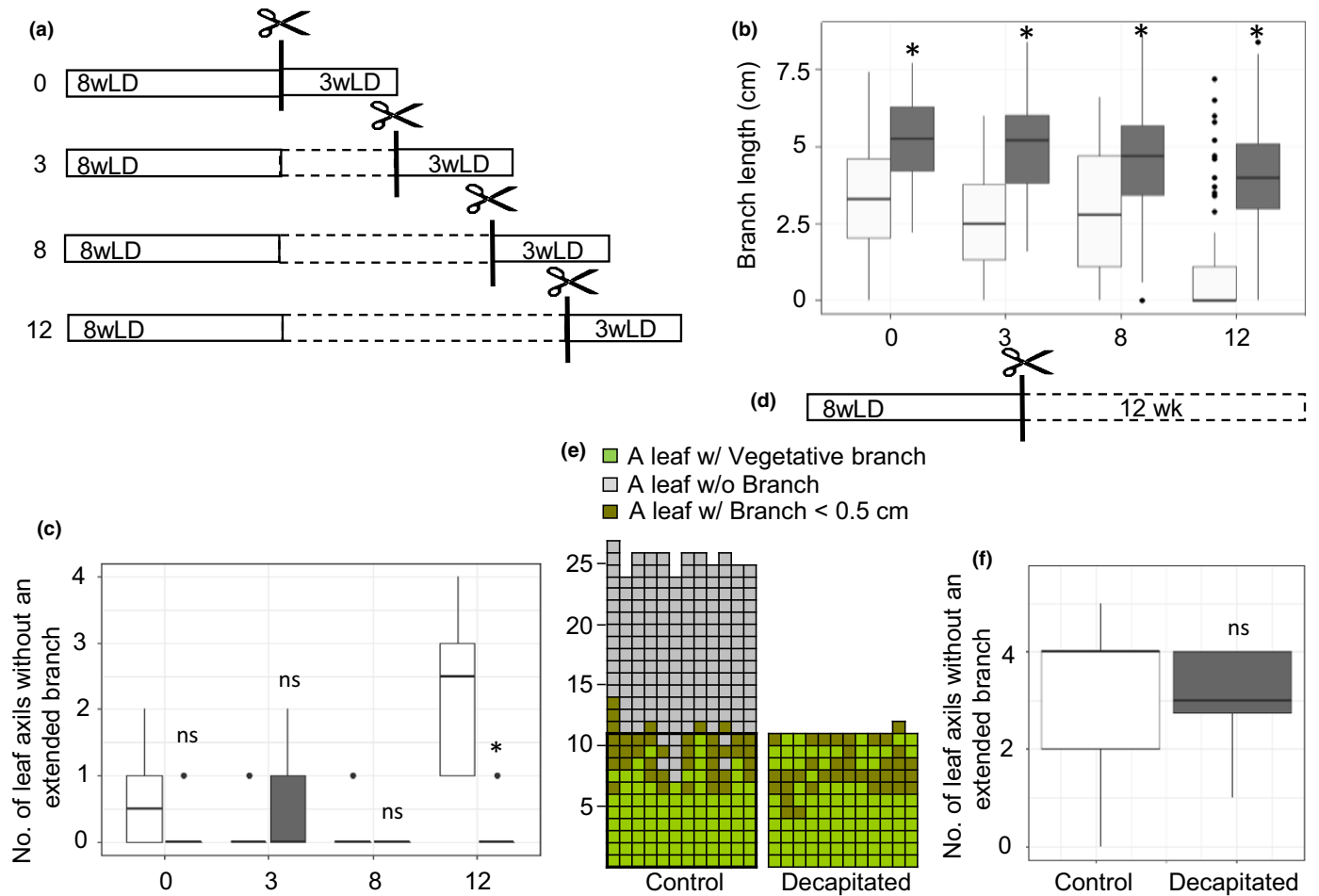


**Fig. 5** V2 buds are ecodormant during vernalization. (a–c) Decapitation experiment to assess whether V2 buds are endodormant during cold treatment. (a) Diagram illustrating the experimental design for results obtained from decapitation experiments presented in (b) and (c). *Arabidopsis thaliana* plants were grown for 8 wk in long days (8wLD; solid line box) and subsequently cold treated for 0, 3, 8, and 12 wk (dotted line box). Plants were decapitated before being returned to warm temperatures (solid line box). Control plants are the same as in Fig. 3. (b) Branch length of new branches of control (white) or decapitated plants (gray) was scored 3 wk after decapitation. (c) Number of leaf axes without a branch in control (white) or decapitated plants (gray) scored 3 wk after decapitation. Nodes 1–11 scored for treatment 0; nodes 1–12 scored for treatment 3, nodes 1–13 scored for treatment 8, and nodes 1–14 scored for treatment 12. (d–f) Decapitation experiment to assess whether V2 buds are ecodormant during vernalization. (d) Diagram illustrating the experimental design for results obtained from decapitation experiments presented in (e) and (f). Plants were grown for 8 wk in long days (8wLD) and decapitated before being subjected to 12 wk of cold treatment. (e) Analysis of branch formation in plants at the end of the 12 wk of cold treatment in control and decapitated plants. As in Fig. 2, each column represents a single plant, and each square within a column represents an individual leaf axil numbered from the oldest to the youngest node. Green color indicates the presence of a vegetative axillary branch in the particular leaf axil. Gray or brown colors indicate the absence of an axillary branch or the presence of a branch smaller than 0.5 cm in the particular leaf axil. (f) Number of leaf axes without a branch (represented with brown and gray boxes in e) at the end of 12 wk of cold treatment in control (white) and decapitated plants (gray). Only nodes 1–11 were scored in control plants. The boxes in (c) and (f) indicate the interquartile range, the horizontal line in the middle is the median, the vertical lines (whiskers) correspond to the highest or lowest value within 1.5 times the interquartile range, and the dots are outliers. Asterisks indicate significant differences using Student's *t*-test  $P < 0.05$  between control and decapitated plants.  $n = 12$ . ns, not significant.

12–16 (corresponding to nodes in the V2 zone) (Figs 9a,d,e, Fig. S6). In these two lines, transcript levels of *AaHB53* were reduced in V2 buds at the end of vernalization and post-vernalization but not before vernalization (Fig. S5). Interestingly, transcript accumulation of *AaHIS1-3* and *AaAIRP2* in the 35S: *AaBRC1 dsRNAi* lines was similar to control plants in all developmental stages (Fig. S5). These results suggest that *AaBRC1* regulates the activity of V2 buds during and after vernalization. However, an *AaBRC1*-independent pathway regulating bud dormancy might also exist.

## Discussion

Perennial plants flower multiple times during their life cycle by restricting senescence only to reproductive branches and maintaining growth through vegetative axillary branches and dormant buds. Bud dormancy, in general, serves as a strategy, which is followed by annual and perennial species, to enable plants to regrow after harsh environmental conditions or after damage due to biotic and abiotic cues. In herbaceous plants, buds in the axils of younger leaves that are close to the shoot apical meristem are

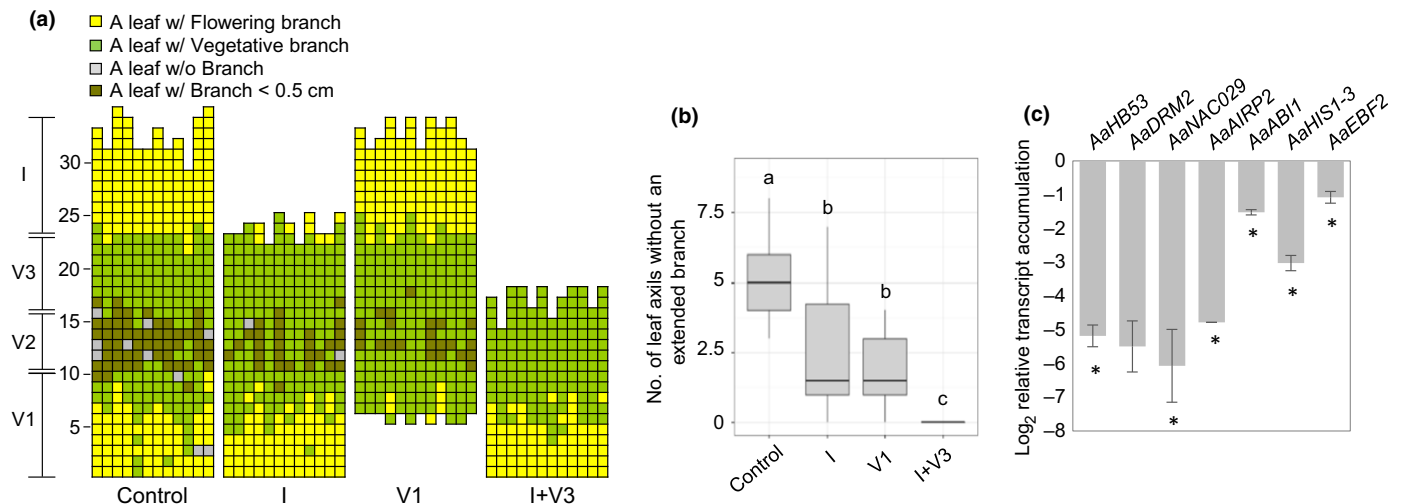


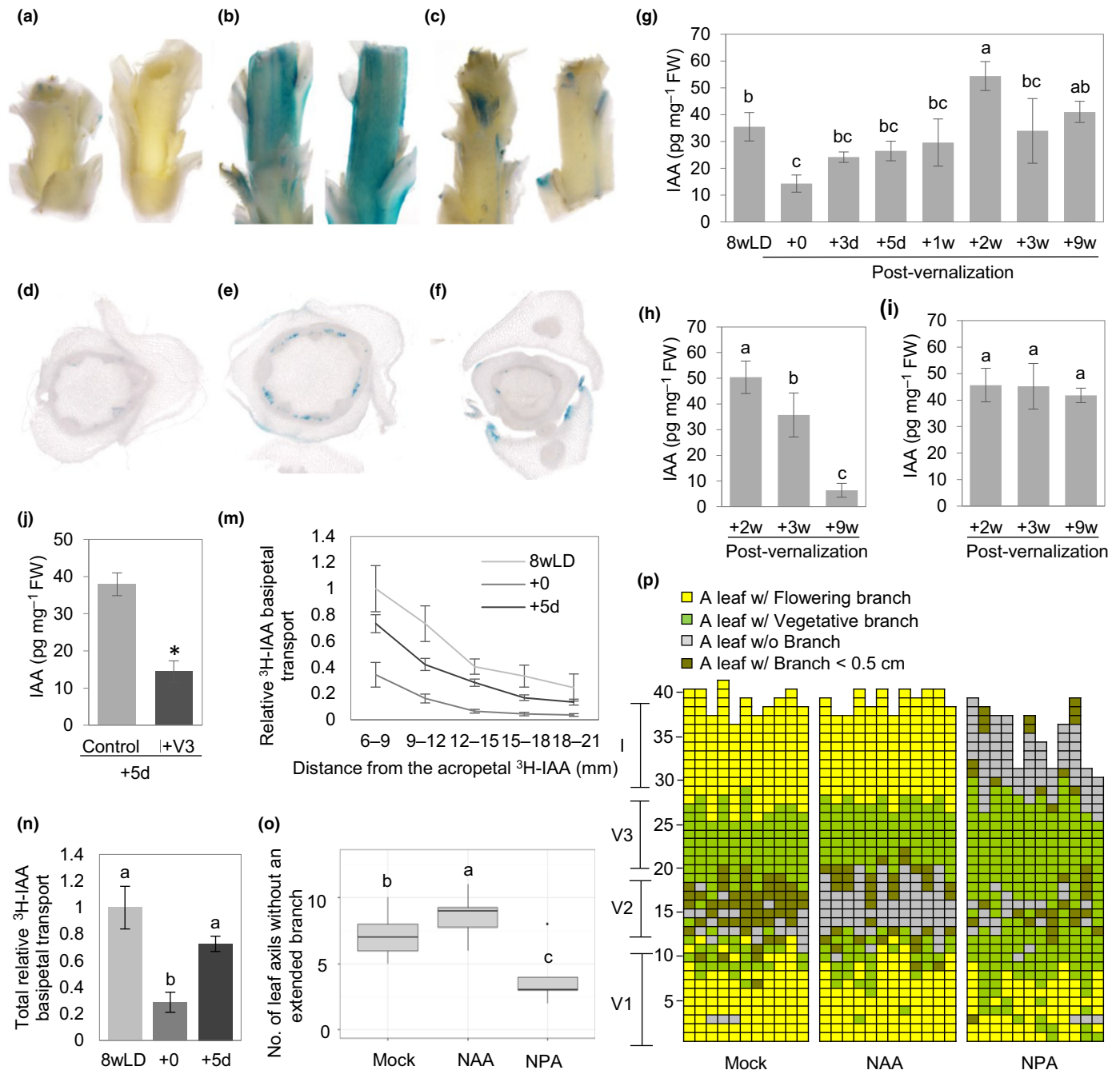
**Fig. 6** Dormancy of V2 buds post-vernalization is regulated by correlative inhibition. (a) Analysis of branch formation after excision of axillary branches or buds belonging to different zones. As in Fig. 5(a) (treatment 12), *Arabidopsis thaliana* plants were decapitated immediately at the end of 12 wk of cold treatment and subsequently moved to a long days (LDs) glasshouse for 3 wk. In all treatments V3 and inflorescence (I) buds were dissected under the binocular. 'Control' indicates intact plants, 'I' indicates plants in which the inflorescence buds have been dissected, 'V1' indicates plants in which V1 branches have been removed, and 'I + V3' indicates plants in which the inflorescence and V3 buds have been dissected. As in Fig. 2, each column represents a single plant and each square within a column represents an individual leaf axil numbered from the oldest to the youngest node. Yellow or green colors indicate the presence of a flowering or vegetative axillary branch in the particular leaf axil. Gray or brown colors indicate the absence of an axillary branch or the presence of a branch smaller than 0.5 cm in the particular leaf axil ( $n = 10$  or 12). (b) Number of leaf axils without a branch (represented with brown and gray boxes in a) after the excision of buds or branches in different zones. Letters show significant differences between conditions ( $P < 0.05$ ,  $n = 3$ ) using ANOVA followed by Tukey's pairwise multiple comparison test. (c) Relative transcript accumulation of *AaHB53*, *AaDRM2*, *AaNAC029*, *AaAIRP2*, *AaABI1*, *AaHIS1-3*, and *AaEBF2* in V2 buds in response to decapitation of inflorescence and V3 buds together (I + V3) compared with the control at 5 d after return to glasshouse conditions. Expression levels of all genes were normalized with *AaPP2A* and *AaUBI10*. The boxes in (b) indicate the interquartile range, the horizontal line in the middle is the median, the vertical lines (whiskers) correspond to the highest or lowest value within 1.5 times the interquartile range, and the dots are outliers. \*,  $P < 0.05$ , significant differences between control and decapitated plants using Student's *t*-test ( $n = 3$ ). Errors indicate SD. *ABI1*, *ABA INSENSITIVE 1*; *AIRP2*, *ABA INSENSITIVE RING PROTEIN 2*; *DRM2*, *DORMANCY ASSOCIATED GENE 2*; *EBF2*, *EIN3-BINDING F BOX PROTEIN 2*; *HB53*, *HOMEODOMAIN 53*; *HIS1-3*, *HISTONE H1-3*; *NAC029*, *NAC DOMAIN CONTAINING PROTEIN 29*.

often temporarily dormant (Kebrom, 2017). This phenomenon is explained by apical dominance, in which, after the removal of the shoot apical meristem, buds can resume growth (Cline, 1991). Apical dominance in trees and shrubs is more complex. In trees the highest buds have the tendency to grow out, whereas in shrubs the lowest buds usually develop into a branch (Cline, 1991). Thus, often dormant axillary buds are not necessarily located in the axils of leaves close to the shoot apical meristem, and leaves with dormant axillary buds in their axils are often older than the ones with flowering or vegetative branches (Costes & Guédon, 2002; Costes *et al.*, 2014; Lazaro *et al.*, 2018). Nevertheless, the fate of these buds is still influenced by other parts of the plant (Costes *et al.*, 2014).

We demonstrated that a major factor that determines the complex shoot architecture and the positioning of dormant buds along the shoot is flowering. Specifically, the separation in time of the different steps of flowering (floral induction, flower bud initiation, and anthesis), which is seen in many perennial species, is crucial for shaping a complex shoot architecture. Perennials often initiate floral buds before winter, either during the summer or early autumn, and flower the following spring (Vasconcelos *et al.*, 2009; Hsu *et al.*, 2011; Koskela *et al.*, 2012; Kurokura *et al.*, 2013). Wild-type *A. alpina* plants initiate flower buds during cold treatment and flower rapidly after subsequent exposure to growth-promoting conditions (Wang *et al.*, 2009). V2 axillary

buds that stay stably dormant are formed before the onset of vernalization (Ponraj & Theres, 2020). In this study, we show that, irrespective of what happens to the shoot apical meristem, V2 buds become ecodormant during cold exposure. Floral bud initiation during cold treatment determines the fate of V2 buds at later developmental stages, after plants have been exposed again to growth-promoting conditions.

In annuals, and certainly in some perennial species, the induction to flowering changes the pattern of axillary bud initiation (from acropetal to basipetal), and new buds are initiated in leaf axils adjacent to the shoot apical meristem (Prusinkiewicz *et al.*, 2009; Dierck *et al.*, 2016). In perennials, these buds do not commit to reproductive development and the following year give rise to vegetative structures (Carmona *et al.*, 2002; Foster *et al.*, 2003). As *A. alpina* plants initiate flowering during vernalization, new buds (V3) are initiated during cold exposure and are designated to ensure the maintenance of vegetative growth after flowering, giving rise to vegetative axillary branches (Wang *et al.*, 2009; Ponraj & Theres, 2020). Maintenance of vegetative growth in V3 branches is ensured by the floral repressor PERPETUAL FLOWERING 1 (PEP1), as *PEP1* mRNA levels are upregulated in the V3 branches after vernalization irrespective of the duration of cold treatment (Wang *et al.*, 2009; Lazaro *et al.*, 2018). We showed that flowering in the main shoot apex is always linked to the presence of the V3 vegetative axillary



branches. In addition, the transcripts of genes previously shown to correlate with the release of bud dormancy are already enhanced in V3 buds during cold exposure (Devitt & Stafstrom, 1995; Campbell *et al.*, 1996; Horvath *et al.*, 2002; Freeman *et al.*, 2003). These results suggest that V3 buds are not dormant during and after cold exposure. Similarly, in tulip bulbs, axillary buds located close to the flowering shoot apex never arrest growth (Moreno-Pachon *et al.*, 2018). The link between flowering and paradormancy has been demonstrated in rice, in which the flowering time regulator *Heading date 3a*, the orthologue of *FLOWERING LOCUS T* in *A. thaliana*, acts as the systemic signal for flowering and axillary bud activation (Tsuji *et al.*, 2015).

In *A. alpina*, the flowering time regulator PEP1 might orchestrate the crosstalk between flowering and bud activity, as the *pep1-1* mutant has a clear branching phenotype. In rice, it has also been shown that another flowering time regulator, the transcription factor SQUAMOSA PROMOTER BINDING PROTEIN-LIKE 14 (OsSPL14), which is the orthologue of SPL15, regulates shoot branching and panicle branching (Miura *et al.*, 2010). However, this role of SPL15 is not conserved in *A. alpina*, as the activity of V2 buds is not affected in *Aaspl15*-knockout lines (Hyun *et al.*, 2019).

Flowering might indirectly determine the fate of V2 buds by simply giving an advantage to the inflorescence and V3 buds



**Fig. 7** Auxin response, endogenous indole-3-acetic acid (IAA) level and IAA transport capacity in the V2 main stem is decreased during vernalization and is increased post-vernalization. Modification of this pattern changes the size of the V2 zone. (a–f)  $\beta$ -Glucuronidase activity within the V2 region on the main stem. (a) V2 main stem region at the end of vernalization. (b) V2 main stem region at 5 d post-vernalization. (c) V2 main stem region at 5 d post-vernalization in plants in which the inflorescence and V3 buds were dissected immediately at the end of the 12 wk of cold treatment (see also Fig. 5a). (d) Transversal section of V2 main stem region at the end of vernalization. (e) Transversal section of V2 main stem region at 5 d post-vernalization. (f) Transversal section of V2 main stem at 5 d post-vernalization in plants in which the inflorescence and V3 buds were dissected immediately at the end of the 12 wk of cold treatment (see also Fig. 5a). (g–j) IAA level: (g) in V2 main stem region before vernalization (8wLD), at the end of vernalization (+0), 3 and 5 d (+3d and +5d), and 1, 2, 3, and 9 wk post-vernalization (+1w, +2w, +3w, and +9w); (h) at the base of the inflorescence stem; (i) at the base of the V3 axillary vegetative branches; (j) in V2 main stem region in plant in which the inflorescence and V3 buds have been dissected immediately at the end of the 12 wk of cold treatment; \*,  $P < 0.05$ , significant difference between control and decapitated plants using Student's  $t$ -test ( $n = 3$ ). Samples were harvested from plants transferred to a long day (LD) glasshouse 5 d after decapitation. Letters indicate significant differences between conditions ( $P < 0.05$ ,  $n = 3$ ) using ANOVA followed by Tukey's pairwise multiple comparison test. Errors indicate SD. (m,n) IAA transport capacity in V2 main stem region in 8-wk-old plants grown in LD (8wLD), at the end of vernalization (+0), and 5 d post-vernalization (+5d): (m)  $^3\text{H}$ -IAA measured in millimeters of stem from the  $^3\text{H}$ -IAA acropetal source relative to the  $^3\text{H}$ -IAA measured in the 6–9 mm of stems from 8wLD plants; (n) total  $^3\text{H}$ -IAA in stem (6–21 mm) at the end of vernalization (0) and 5 d after vernalization (5d) relative to the  $^3\text{H}$ -IAA in stems from 8wLD plants. Letters indicate significant differences between conditions ( $P < 0.05$ ,  $n = 3$ ) using ANOVA followed by Tukey's pairwise multiple comparison test. Errors indicate SE. (o) Number of leaf axils without a branch (represented with brown and gray boxes in p) in *Arabidopsis thaliana* plants vernalized for 12 wk and subsequently sprayed with mock, 100  $\mu\text{M}$  1-naphthaleneacetic acid (NAA) or 100  $\mu\text{M}$  1-N-naphthylphthalamic acid (NPA) immediately at the end of 12 wk of cold treatment and 1 wk after the return to glasshouse conditions. Plants were scored 5 wk after they were returned to the glasshouse. Letters indicate significant differences between conditions ( $P < 0.05$ ,  $n = 12$ ) using ANOVA followed by using Tukey's pairwise multiple comparison test. (p) Analysis of branch formation after mock, NAA, or NPA treatment. Branch scoring is presented as in Fig. 2. Each column represents a single plant and each square within a column represents an individual leaf axil numbered from the oldest to the youngest node. Yellow or green colors indicate the presence of a flowering or vegetative axillary branch in the particular leaf axil. Gray or brown colors indicate the absence of an axillary branch or the presence of a branch smaller than 0.5 cm in the particular leaf axil. The boxes in (o) indicate the interquartile range, the horizontal line in the middle is the median, the vertical lines (whiskers) correspond to the highest or lowest value within 1.5 times the interquartile range, and the dots are outliers.

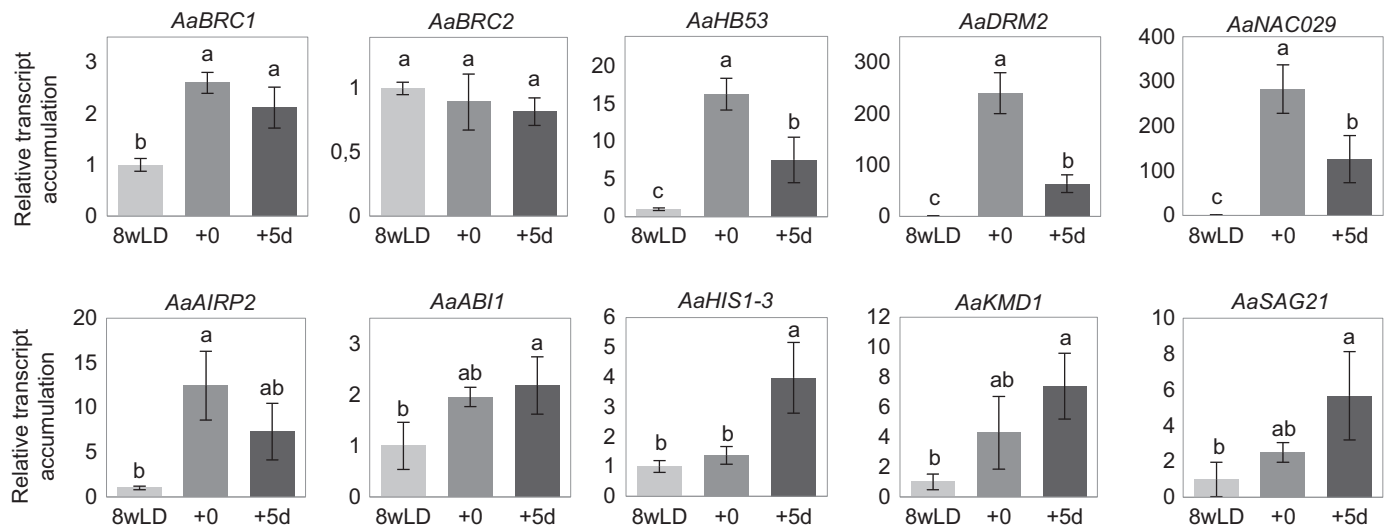


**Fig. 8** Transcript accumulation of dormancy related genes in *Arabidopsis thaliana* V2 buds is increased during and maintained post-vernalization. Relative transcript accumulation of *AaBRC1*, *AaBRC2*, *AaHB53*, *AaDRM2*, *AaNAC029*, *AaAIRP2*, *AaABI1*, *AaHIS1-3*, *AaKMD1*, and *AaSAG21* in 8-wk-old plants grown in long days (LDs) (8wLD; light gray), at the end of vernalization (+0; gray), and 5 d after vernalization (+5d, dark gray). Transcript levels of all genes are normalized with *AaPP2A* and *AaUBI10*. ( $n = 3$ .) Letters indicate significant differences between conditions ( $P < 0.05$ ,  $n = 3$ ) using ANOVA followed by using Tukey's pairwise multiple comparison test. Errors indicate SD. *ABI1*, *ABA INSENSITIVE 1*; *AIRP2*, *ABA INSENSITIVE RING PROTEIN 2*; *BRC1* and *2*, *BRANCHED 1* and *2*; *DRM2*, *DORMANCY ASSOCIATED GENE 2*; *HB53*, *HOMEODOMAIN 53*; *HIS1-3*, *HISTONE H1-3*; *KMD1*, *KISS ME DEADLY 1*; *NAC029*, *NAC DOMAIN CONTAINING PROTEIN 29*; *SAG21*, *SENESCENCE-ASSOCIATED GENE 21*.

formed during cold treatment to outgrow rapidly when plants experience growth-promoting conditions. Consequently, the development of these buds might be at the expense of the V2 buds. V3 branches and the inflorescence may act as strong nutrient sinks during and after vernalization, causing sugar diversion from the V2 buds and thereby contributing to growth inhibition. This is in line with the fact that *BRC1* is inhibited by sugars in both perennials and annuals and that carbon-starvation-induced dormancy is observed in annual and perennial plants (Mason *et al.*, 2014;

Barbier *et al.*, 2015; Tarancón *et al.*, 2017). From the transcript levels of dormancy marker genes and our physiological studies, we can conclude that dormancy in V2 buds is enhanced during vernalization and is maintained post-vernalization. After the return to warm temperatures, V2 buds enter a latent state, mainly being dominated by the inflorescence and V3 branches. The auxin canalization model postulates that polar auxin transport from an apical auxin source inhibits sufficient polar auxin stream from lateral buds (Prusinkiewicz *et al.*, 2009). In our system, the fact that

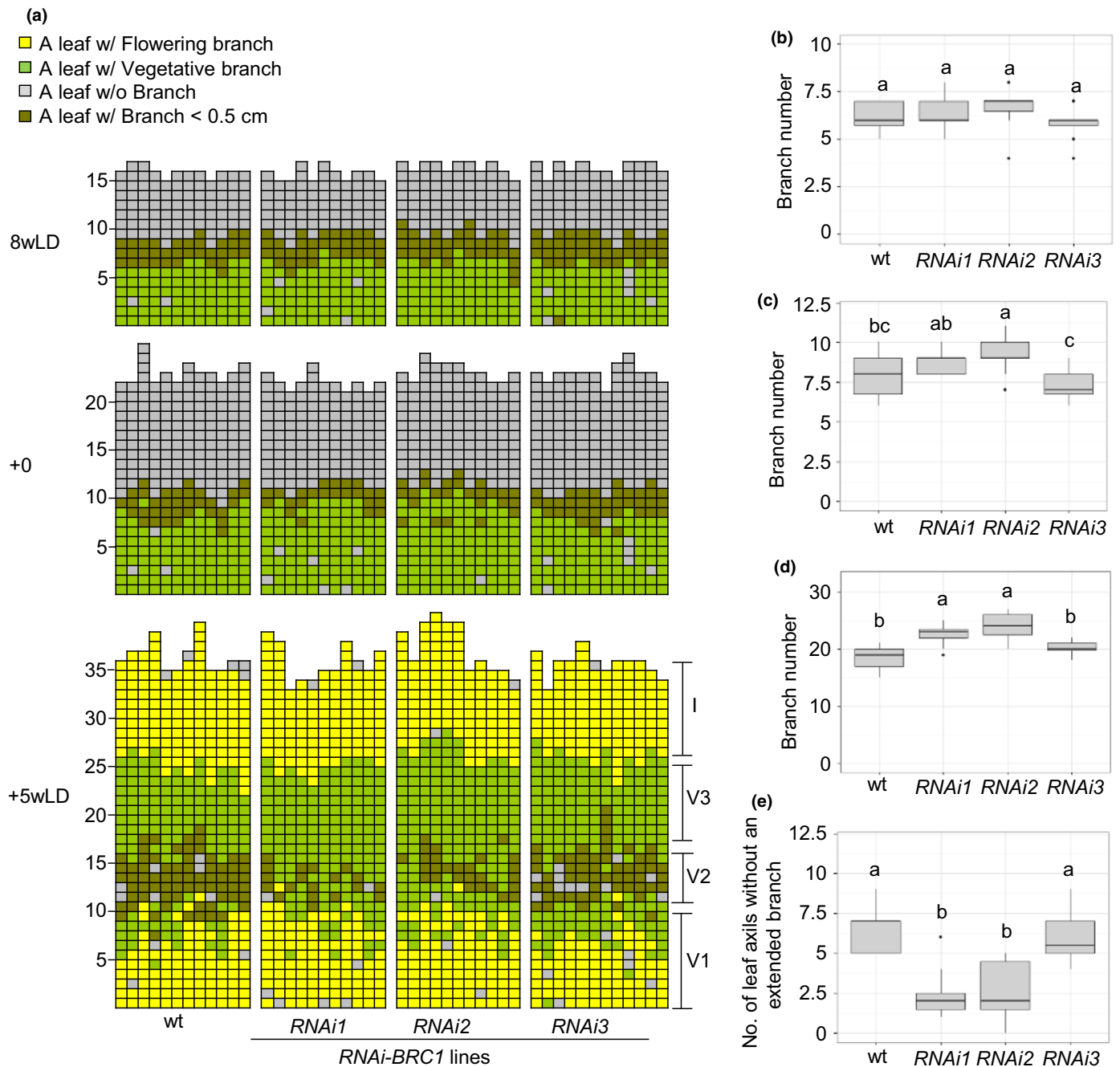


**Fig. 9** AaBRC1 ensures the maintenance of dormancy in V2 buds post-vernialization. (a) Analysis of branch formation in wild-type (wt) *Arabis alpina* plants and in 35S:AaBRC1 dsRNAi lines 1 to 3 in 8-wk-old plants grown in long days (LDs) (8wLD), at the end of vernalization (+0), and 5 wk post-vernialization (+5wLD). As in Fig. 2, each column represents a single plant and each square within a column represents an individual leaf axil numbered from the oldest to the youngest node. Yellow or green colors indicate the presence of a flowering or vegetative axillary branch in the particular leaf axil. Grey or brown colors indicate the absence of an axillary branch or the presence of a branch smaller than 0.5 cm in the particular leaf axil.  $n = 12$ . (b) Branch number per plant in 8-wk-old plants grown in LDs (8wLD). (c) Branch number per plant in plants at the end of vernalization (+0). (d) Branch number per plant in plants at 5 wk after vernalization (+5wLD). (e) Number of leaf axils without a branch at 5 wk after vernalization (+5w; represented with brown and gray boxes in a). The boxes in (b–e) indicate the interquartile range, the horizontal line in the middle is the median, the vertical lines (whiskers) correspond to the highest or lowest value within 1.5 times the interquartile range, and the dots are outliers. Letters indicate significant differences between conditions ( $P < 0.05$ ) using ANOVA followed by using Tukey's pairwise multiple comparison test. BRC1, BRANCHED 1; ds, double-stranded; RNAi, RNA interference.

V3 vegetative branches are positioned in the axils of the leaves just above the V2 zone might not be random, and they might act as an auxin source to determine the activity of V2 buds. This is in line

with our results, as we observed enhancement of basipetal auxin transport, increased auxin response, and endogenous IAA levels in the stem after vernalization.

Our study links the pattern of flowering observed in temperate perennials with the maintenance of dormant buds across multiple seasons and provides the framework of how perennials ensure long-term growth.






## Acknowledgements

MCA acknowledges support from the Deutsche Forschungsgemeinschaft (German Research Foundation) under Germany's Excellence Strategy – EXC 2048/1 – Project ID: 390686111. KL acknowledges support from the Knut and Alice Wallenberg Foundation, the Swedish Research Council, and the Swedish Governmental Agency for Innovation Systems. We would like to thank Roger Granbom, Udhaya Ponraj, Lisa Clark, Julia Benecke, Vicky Tilmes, Kirstin Krause and Panpan Jiang for technical assistance or for sharing primers, Rainer Häusler and Stan Kopriva for discussions regarding the auxin transport assay, and Klaus Theres, George Coupland and Margaret Kox for the critical reading of the manuscript.

## Author contributions

AV, PM and MCA planned and designed the research, AV, AR, KL and UN performed experiments, AV, PM, AR and MCA analyzed data, and AV and MCA wrote the manuscript. PM and AR contributed equally to this work.

## ORCID

Maria C. Albani  <https://orcid.org/0000-0002-8215-020X>  
 Karin Ljung  <https://orcid.org/0000-0003-2901-189X>  
 Priyanka Mishra  <https://orcid.org/0000-0003-1798-2306>  
 Ulla Neumann  <https://orcid.org/0000-0001-9200-4209>  
 Alice Vayssières  <https://orcid.org/0000-0002-8625-2879>

## References

- Aguilar-Martínez JA, Poza-Carrión C, Cubas P. 2007. *Arabidopsis* *BRANCHED1* acts as an integrator of branching signals within axillary buds. *The Plant Cell* 19: 458–472.
- Andersen SU, Buechel S, Zhao Z, Ljung K, Novak O, Busch W, Schuster C, Lohmann JU. 2008. Requirement of B2-type *Cyclin-Dependent Kinases* for meristem integrity in *Arabidopsis thaliana*. *The Plant Cell* 20: 88–100.
- Arite T, Umehara M, Ishikawa S, Hanada A, Maekawa M, Yamaguchi S, Kyozuka J. 2009. *d14*, a strigolactone-insensitive mutant of rice, shows an accelerated outgrowth of tillers. *Plant and Cell Physiology* 50: 1416–1424.
- Arora R, Rowland LJ, Tanino K. 2003. Induction and release of bud dormancy in woody perennials: a science comes of age. *HortScience* 38: 911–921.
- Barbier F, Péron T, Lecerf M, Perez-García MD, Barrière Q, Rolčík J, Boutet-Mercey S, Citerne S, Lemoine R, Porcheron B *et al.* 2015. Sucrose is an early modulator of the key hormonal mechanisms controlling bud outgrowth in *Rosa hybrida*. *Journal of Experimental Botany* 66: 2569–2582.
- Campbell MA, Suttle JC, Sell TW. 1996. Changes in cell cycle status and expression of p34<sup>cdc2</sup> kinase during potato tuber meristem dormancy. *Physiologia Plantarum* 98: 743–752.
- Carmona MJ, Cubas P, Martínez-Zapater JM. 2002. *VFL*, the grapevine *FLORICAULA/LEAFY* ortholog, is expressed in meristematic regions independently of their fate. *Plant Physiology* 130: 68–77.
- Chao WS, Doğramacı M, Horvath DP, Anderson JV, Foley ME. 2017. Comparison of phytohormone levels and transcript profiles during seasonal dormancy transitions in underground adventitious buds of leafy spurge. *Plant Molecular Biology* 94: 281–302.
- Cline MG. 1991. Apical dominance. *The Botanical Review* 57: 318–358.
- Clough SJ, Bent AF. 1998. Floral dip: a simplified method for *Agrobacterium*-mediated transformation of *Arabidopsis thaliana*. *The Plant Journal* 16: 735–743.
- Considine MJ, Considine JA. 2016. On the language and physiology of dormancy and quiescence in plants. *Journal of Experimental Botany* 67: 3189–3203.
- Costes E, Crespel L, Denoyes B, Morel P, Demene M-N, Lauri P-E, Wenden B. 2014. Bud structure, position and fate generate various branching patterns along shoots of closely related Rosaceae species: a review. *Frontiers in Plant Science* 5: e666.
- Costes E, Guédon Y. 2002. Modelling branching patterns on 1-year-old trunks of six apple cultivars. *Annals of Botany* 89: 513–524.
- Crawford S, Shinohara N, Sieberer T, Williamson L, George G, Hepworth J, Müller D, Domagalska MA, Leyser O. 2010. Strigolactones enhance competition between shoot branches by dampening auxin transport. *Development* 137: 2905–2913.
- Destefano-Beltrán L, Knauber D, Huckle L, Suttle JC. 2006. Effects of postharvest storage and dormancy status on ABA content, metabolism, and expression of genes involved in ABA biosynthesis and metabolism in potato tuber tissues. *Plant Molecular Biology* 61: 687–697.
- Devitt ML, Stafstrom JP. 1995. Cell cycle regulation during growth–dormancy cycles in pea axillary buds. *Plant Molecular Biology* 29: 255–265.
- Dierck R, De Keyser E, De Riek J, Dhooche E, Van Huylenbroeck J, Prinsen E, Van Der Straeten D. 2016. Change in auxin and cytokinin levels coincides with altered expression of branching genes during axillary bud outgrowth in chrysanthemum. *PLoS ONE* 11: e0161732.
- Fortino V, Greco D. 2015. Bubble chart to compare biological annotations by using DAVID. [WWW document] URL <https://cran.r-project.org/web/packages/BACA/index>.
- Foster T, Johnston R, Seleznyova A. 2003. A morphological and quantitative characterization of early floral development in apple (*Malus × domestica* Borkh.). *Annals of Botany* 92: 199–206.
- Freeman D, Riou-Khamlichi C, Oakenfull EA, Murray JAH. 2003. Isolation, characterization and expression of cyclin and cyclin-dependent kinase genes in Jerusalem artichoke (*Helianthus tuberosus* L.). *Journal of Experimental Botany* 54: 303–308.
- González-Grandío E, Pajoro A, Franco-Zorrilla JM, Tarancón C, Immink RGH, Cubas P. 2017. Abscisic acid signaling is controlled by a *BRANCHED1/HD-ZIP1* cascade in *Arabidopsis* axillary buds. *Proceedings of the National Academy of Sciences, USA* 114: E245–E254.
- González-Grandío E, Poza-Carrión C, Sorzano COS, Cubas P. 2013. *BRANCHED1* promotes axillary bud dormancy in response to shade in *Arabidopsis*. *The Plant Cell* 25: 834–850.
- Holalu SV, Finlayson SA. 2017. The ratio of red light to far red light alters *Arabidopsis* axillary bud growth and abscisic acid signalling before stem auxin changes. *Journal of Experimental Botany* 68: 943–952.
- Horvath DP, Chao WS, Anderson JV. 2002. Molecular analysis of signals controlling dormancy and growth in underground adventitious buds of leafy spurge. *Plant Physiology* 128: 1439–1446.
- Hsu C-Y, Adams JP, Kim H, No K, Ma C, Strauss SH, Drnevich J, Vandervelde L, Ellis JD, Rice BM *et al.* 2011. *FLOWERING LOCUS T* duplication coordinates reproductive and vegetative growth in perennial poplar. *Proceedings of the National Academy of Sciences, USA* 108: 10756–10761.
- Huang DW, Sherman BT, Lempicki RA. 2009. Systematic and integrative analysis of large gene lists using DAVID bioinformatics resources. *Nature Protocols* 4: 44–57.
- Hyun Y, Vincent C, Tilmes V, Bergonzi S, Martínez-Gallegos R, Severing E. 2019. A regulatory circuit conferring varied flowering response to cold in annual and perennial plants. *Science* 363: 409–412.
- Kebrom TH. 2017. A growing stem inhibits bud outgrowth – the overlooked theory of apical dominance. *Frontiers in Plant Science* 8: e1874.

- Kim HJ, Chiang Y, Kieber JJ, Schaller GE. 2013. SCF<sup>KMD</sup> controls cytokinin signaling by regulating the degradation of type-B response regulators. *Proceedings of the National Academy of Sciences, USA* 110: 10028–10033.
- Koskela EA, Mouhu K, Albani MC, Kurokura T, Rantanen M, Sargent DJ, Battey NH, Coupland G, Elomaa P, Hytonen T. 2012. Mutation in *TERMINAL FLOWER1* reverses the photoperiodic requirement for flowering in the wild strawberry *Fragaria vesca*. *Plant Physiology* 159: 1043–1054.
- Kurokura T, Mimida N, Battey NH, Hytonen T. 2013. The regulation of seasonal flowering in the Rosaceae. *Journal of Experimental Botany* 64: 4131–4141.
- Lang GA, Early JD, Martin GC, Darnell RL. 1987. Endo, para, and ecodormancy: physiological terminology and classification for dormancy research. *HortScience* 22: 371–377.
- Lazaro A, Obeng-Hinneh E, Albani MC. 2018. Extended vernalization regulates inflorescence fate in *Arabidopsis thaliana* by stably silencing *PERPETUAL FLOWERING1*. *Plant Physiology* 176: 2819–2833.
- Lewis DR, Muday GK. 2009. Measurement of auxin transport in *Arabidopsis thaliana*. *Nature Protocols* 4: 437–451.
- Mason MG, Ross JJ, Babst BA, Wienclaw BN, Beveridge CA. 2014. Sugar demand, not auxin, is the initial regulator of apical dominance. *Proceedings of the National Academy of Sciences, USA* 111: 6092–6097.
- Michaels SD, Amasino RM. 1999. *FLOWERING LOCUS C* encodes a novel MADS domain protein that acts as a repressor of flowering. *The Plant Cell* 11: 949–956.
- Miura K, Ikeda M, Matsubara A, Song XJ, Ito M, Asano K, Matsuoka M, Kitano H, Ashikari M. 2010. *OsSPL14* promotes panicle branching and higher grain productivity in rice. *Nature Genetics* 42: 545–549.
- Moreno-Pachon NM, Mutimawurugo MC, Heynen E, Sergeeva L, Benders A, Blilou I, Hilhorst HWM, Immink RGH. 2018. Role of *Tulipa gesneriana* *TEOSINTE BRANCHED1* (*TgTBI*) in the control of axillary bud outgrowth in bulbs. *Plant Reproduction* 31: 145–157.
- Nilsson P, Tuomi J, Astrom M. 1996. Bud dormancy as a bet-hedging strategy. *American Naturalist* 147: 269–281.
- Paponov IA, Paponov M, Teale W, Menges M, Chakrabortee S, Murray JAH, Palme K. 2008. Comprehensive transcriptome analysis of auxin responses in *Arabidopsis*. *Molecular Plant* 1: 321–337.
- Pfaffl MW. 2001. A new mathematical model for relative quantification in real-time RT-PCR. *Nucleic Acids Research* 29: 2002–2007.
- Ponraj U, Theres K. 2020. Keep a distance to be different: axillary buds initiating at a distance from the shoot apical meristem are crucial for the perennial life style of *Arabidopsis thaliana*. *New Phytologist*. doi: 10.1111/nph.16512.
- Prusinkiewicz P, Crawford S, Smith RS, Ljung K, Bennett T, Ongaro V, Leyser O. 2009. Control of bud activation by an auxin transport switch. *Proceedings of the National Academy of Sciences, USA* 106: 17431–17436.
- Rameau C, Bertheloot J, Leduc N, Andrieu B, Foucher F, Sakr S. 2015. Multiple pathways regulate shoot branching. *Frontiers in Plant Science* 5: e741.
- Rohde A, Bhalerao RP. 2007. Plant dormancy in the perennial context. *Trends in Plant Science* 12: 217–223.
- Roman H, Girault T, Barbier F, Péron T, Brouard N, Pěňčík A, Novák O, Vian A, Sakr S, Lothier J *et al.* 2016. Cytokinins are initial targets of light in the control of bud outgrowth. *Plant Physiology* 172: 489–509.
- Scarpella E, Francis P, Berleth T. 2004. Stage-specific markers define early steps of procambium development in *Arabidopsis* leaves and correlate termination of vein formation with mesophyll differentiation. *Development* 131: 3445–3455.
- Sharova EI. 2007. Expansins: proteins involved in cell wall softening during plant growth and morphogenesis. *Russian Journal of Plant Physiology* 54: 713–727.
- Sheldon CC, Rouse DT, Finnegan EJ, Peacock WJ, Dennis ES. 2000. The molecular basis of vernalization: the central role of *FLOWERING LOCUS C* (*FLC*). *Proceedings of the National Academy of Sciences, USA* 97: 3753–3758.
- Shinohara N, Taylor C, Leyser O. 2013. Strigolactone can promote or inhibit shoot branching by triggering rapid depletion of the auxin efflux protein PIN1 from the plasma membrane. *PLoS Biology* 11: e1001474.
- Singh RK, Maurya JP, Azeez A, Miskolczi P, Tylewicz S, Stojković K, Delhomme N, Busov V, Bhalerao RP. 2018. A genetic network mediating the control of bud break in hybrid aspen. *Nature Communications* 9: e4173.
- Snow R. 1925. The correlative inhibition of the growth of axillary buds. *Annals of Botany* 39: 841–859.
- Tarancón C, González-Grandío E, Oliveros JC, Nicolas M, Cubas P. 2017. A conserved carbon starvation response underlies bud dormancy in woody and herbaceous species. *Frontiers in Plant Science* 8: e788.
- Tsuji H, Tachibana C, Tamaki S, Taoka K, Kyoizuka J, Shimamoto K. 2015. Hd3a promotes lateral branching in rice. *The Plant Journal* 82: 256–266.
- Vasconcelos CM, Greven M, Winefield CS, Trought MCT, Raw V. 2009. The flowering process of *Vitis vinifera*: a review. *American Journal of Enology and Viticulture* 60: 411–434.
- Wang B, Smith SM, Li J. 2018. Genetic regulation of shoot architecture. *Annual Review of Plant Biology* 69: 437–468.
- Wang R, Farrona S, Vincent C, Joecker A, Schoof H, Turck F, Alonso-Blanco C, Coupland G, Albani MC. 2009. *PEP1* regulates perennial flowering in *Arabidopsis thaliana*. *Nature* 459: 423–427.
- Waters MT, Nelson DC, Scaffidi A, Flematti GR, Sun YK, Dixon KW, Smith SM. 2012. Specialisation within the DWARF14 protein family confers distinct responses to karrikins and strigolactones in *Arabidopsis*. *Development* 139: 1285–1295.
- Werner T, Motyka V, Strnad M, Schmullig T. 2001. Regulation of plant growth by cytokinin. *Proceedings of the National Academy of Sciences, USA* 98: 10487–10492.
- Zhao Y, Christensen SK, Fankhauser C, Cashman JR, Cohen JD, Weigel D, Chory J. 2001. A role for flavin monooxygenase-like enzymes in auxin biosynthesis. *Science* 291: 306–309.
- Zheng C, Halaly T, Acheampong AK, Takebayashi Y, Jikumaru Y, Kamiya Y, Or E. 2015. Abscisic acid (ABA) regulates grape bud dormancy, and dormancy release stimuli may act through modification of ABA metabolism. *Journal of Experimental Botany* 66: 1527–1542.

## Supporting Information

Additional Supporting Information may be found online in the Supporting Information section at the end of the article.

**Fig. S1** Duration of cold treatment influences floral commitment in the shoot apical meristem.

**Fig. S2** GO enrichment analysis in differentially regulated genes in V2 and V3 buds at the end of vernalization (+0) and 5 d after vernalization (+5d).

**Fig. S3** *GUS* transcript accumulation in transgenic *DR5:GUS A. thaliana* lines.

**Fig. S4** *AaBRC1* is the homolog of the *A. thaliana* *BRC1* and its expression is downregulated in response to decapitation.

**Fig. S5** Transcript accumulation of dormancy-associated genes is reduced after vernalization in *35S:AaBRC1 dsRNAi* lines.

**Fig. S6** *35S:AaBRC1 dsRNAi* lines do not show major differences in branch length and total leaf number at flowering.

**Table S1** Primers used in this article.

**Table S2** List of genes whose transcript levels have been identified to be differentially expressed between V2 and V3 buds at the end of vernalization (+0) and 5 d post-vernalization (+5d).

**Table S3** GO enrichment categories identified in genes whose transcript levels have been identified to be differentially expressed



between V2 and V3 buds at the end of vernalization (+0) and 5 d post-vernalization (+5d).

**Table S4** List of coexpressed clusters obtained after hierarchical clustering of the transcript accumulated in V2 and V3 buds at the end of vernalization (+0) and 5 d post-vernalization (+5d).

**Table S5** GO enrichment categories identified in the different coexpressed clusters.

**Table S6** Homologs of *A. thaliana* genes identified as a 'bud dormancy' genes in Tarancón *et al.* (2017) differentially regulated in our transcriptome analysis.

Please note: Wiley Blackwell are not responsible for the content or functionality of any Supporting Information supplied by the authors. Any queries (other than missing material) should be directed to the *New Phytologist* Central Office.



## About *New Phytologist*

- *New Phytologist* is an electronic (online-only) journal owned by the New Phytologist Trust, a **not-for-profit organization** dedicated to the promotion of plant science, facilitating projects from symposia to free access for our Tansley reviews and Tansley insights.
- Regular papers, Letters, Research reviews, Rapid reports and both Modelling/Theory and Methods papers are encouraged. We are committed to rapid processing, from online submission through to publication 'as ready' via *Early View* – our average time to decision is <26 days. There are **no page or colour charges** and a PDF version will be provided for each article.
- The journal is available online at Wiley Online Library. Visit **www.newphytologist.com** to search the articles and register for table of contents email alerts.
- If you have any questions, do get in touch with Central Office (np-centraloffice@lancaster.ac.uk) or, if it is more convenient, our USA Office (np-usaoffice@lancaster.ac.uk)
- For submission instructions, subscription and all the latest information visit **www.newphytologist.com**